AEDC-TR-65-124

IMPROVED METHODS FOR DETERMINING SECOND-THROAT DIFFUSER PERFORMANCE OF ZERO-SECONDARY-FLOW EJECTOR SYSTEMS

R. C. German and J. H. Panesci

ARO, Inc.

July 1965

ROCKET TEST FACILITY
ARNOLD ENGINEERING DEVELOPMENT CENTER
AIR FORCE SYSTEMS COMMAND
ARNOLD AIR FORCE STATION, TENNESSEE

NOTICES

When U. S. Government drawings specifications, or other data are used for any purpose other than a definitely related Government procurement operation, the Government thereby incurs no responsibility nor any obligation whatsoever, and the fact that the Government may have formulated, furnished, or in any way supplied the said drawings, specifications, or other data, is not to be regarded by implication or otherwise, or in any manner licensing the holder or any other person or corporation, or conveying any rights or permission to manufacture, use, or sell any patented invention that may in any way be related thereto.

Qualified users may obtain copies of this report from the Defense Documentation Center.

References to named commercial products in this report are not to be considered in any sense as an endorsement of the product by the United States Air Force or the Government.

Defense Documentation Center release to the Clearinghouse for Federal Scientific and Technical Information (CFSTI) and foreign announcement and distribution of this report are not authorized. The distribution of this report is limited because it contains technology identifiable with items excluded from export by the Department of State.

IMPROVED METHODS FOR DETERMINING SECOND-THROAT DIFFUSER PERFORMANCE OF ZERO-SECONDARY-FLOW EJECTOR SYSTEMS

R. C. German and J. H. Panesci
ARO, Inc.

AF - AEDC
Arnold AFS Tenn

FOREWORD

The results of the research presented were obtained by ARO, Inc. (a subsidiary of Sverdrup and Parcel, Inc.), contract operator of the Arnold Engineering Development Center (AEDC), Air Force Systems Command (AFSC), Arnold Air Force Station, Tennessee, under Contract AF40(600)-1000, Program Element 62405184/6950, Task 695002. The research was conducted from October 1, 1963, to January 1, 1965, under ARO Project No. RW2141 (150141), and the report was submitted by the authors on May 26, 1965.

The authors wish to acknowledge significant assistance received from D. B. Ramsay and J. W. Price (Scientific Computing Branch) in computing the free-jet flow fields on an IBM 7074 computer and from L. F. Smith, Jr. (Research Branch) in the reduction and preparation of the experimental data presented in this report.

This technical report has been reviewed and is approved.

Forrest B. Smith, Jr.
Propulsion Division
DCS/Research

Donald R. Eastman, Jr.
DCS/Research

ABSTRACT

Improved methods are presented for estimating the required starting pressure ratio of a given axisymmetric second-throat, ejector-diffuser system used in rocket altitude simulation. The improved theory involves a more accurate technique for determining ramp pressure. The new technique utilizes the flow field approaching the second throat along with two-dimensional oblique shock relations and the conservation equations to determine the conditions at the throat entrance. The results are applied to second-throat diffusers with throat lengths varying from 0.2 to 8.1 throat diameters and to second throats with a centerbody located at various positions. A comparison of the theoretical starting pressure ratios with the experimental data from previous work, as well as the additional experimental data obtained during this investigation, gave a maximum deviation of less than 10 percent for most of the configurations investigated. The improved method should be especially applicable to ejector-diffuser systems whose nozzle exit flow fields are nonuniform, such as exist in annular and clustered driving nozzles.

CONTENTS

ILLUSTRATIONS

TABLES

NOMENCLATURE

A	Area
C_f	Friction coefficient
D	Diameter
F	Force or impulse function
f	Friction force
h	Height
K_A	Constant used for separation-pressure ratio by Arens-Spiegler

K_M	Constant used for separation-pressure ratio by Mager
L	Length
M	Mach number
$\dot{m}$	Mass flow
N	Number of centerbody vanes
p	Static pressure
p_t	Total pressure
R	Gas constant
r	Radial distance from diffuser centerline
T_t	Total temperature
x	Axial distance
β	Flow angle
γ	Ratio of specific heats
θ	Angle

SUBSCRIPTS

1, 2, 3	Axial stations
a	Annulus
c	Ejector cell or second-throat core
cal	Calculated
℄	Centerline
d	Capture duct
ex	Exhaust
exp	Experimental
i	Impingement section
m	Ramp mid-area
min	Minimum
n	Nozzle
ne	Nozzle exit
oper	Operate
opt	Optimum

R	Ramp section
r	Rake
s	Separated
sp	Spherical
st	Second throat
t	Total
v	Vane support
w	Wall
x	Axial direction
∞	Free-stream conditions

SUPERSCRIPT

*	Nozzle throat

SECTION I
INTRODUCTION

The application of second-throat diffusers in testing of rocket motors at simulated altitude conditions has gained an increasing interest at the Rocket Test Facility (RTF). With the increase in diffuser pressure recovery obtained from a second-throat diffuser, higher altitudes can be simulated by the ejector-action of the rocket exhaust gases with the same facility exhaust machinery.

The investigation of second-throat, ejector-diffuser systems in RTF was reported initially in Ref. 1. Semi-empirical methods were later developed in Ref. 2 to calculate the diffuser starting pressure ratio which gave very good agreement with the experimental results for both long [$(L/D)_{st} > 5$] and short [$(L/D)_{st} < 1$] second-throat ejector systems using conical driving nozzles. The short second-throat theory utilizes the conservation equations to arrive at a one-dimensional supersonic Mach number at the entrance of the minimum area at station 2 (see Fig. 1). The maximum back pressure was then determined which would cause separation of a turbulent boundary layer based on the free, shock-separation criteria proposed by Arens and Spiegler (Ref. 3). The long second-throat theory used the same conservation equations to arrive at the force balance between stations 1 and 2. However, the subsonic solution was used, together with the continuity equation, to calculate the maximum diffuser exit pressure at station 3 for which the long second-throat diffuser will start. Both of these theories involved a semi-empirical method for predicting the pressure drag force on the second-throat ramp, which assumed that the gas expands isentropically from the nozzle throat to the diffuser duct diameter through a mean gas expansion angle, θ_m, as shown in the following sketch.

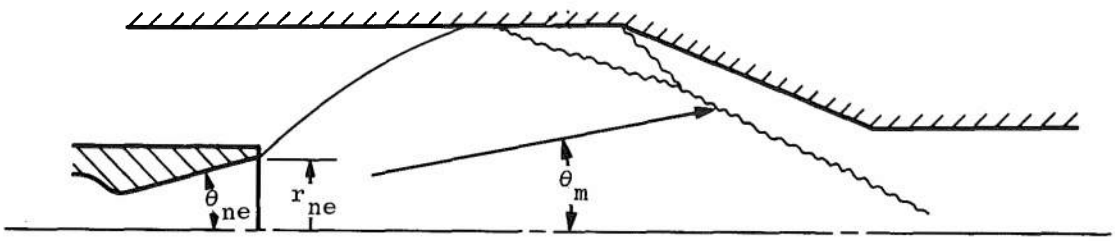

This procedure provides a simple and sufficiently accurate method for predicting the conditions on the ramp and approaching the second-throat entrance for second-throat ejector systems using conical nozzles or nozzles with uniform exit Mach numbers. However, this semi-empirical method is not adequate for annular or cluster nozzles, whose flow conditions at the nozzle exit are highly nonuniform. The investigation was

therefore continued to find a more general approach for calculating the starting pressure ratio of a given second-throat ejector system. A satisfactory theoretical method for determining the performance of such systems was developed, which requires that the flow conditions approaching the second throat be known. The pressure drag force on the second-throat ramp and the conditions at the throat entrance are then determined by using two-dimensional oblique shock relations and the conservation equations. The starting pressure ratio for a given second-throat diffuser configuration can then be calculated by making additional assumptions for the forces imposed downstream of the throat entrance, depending on the type of second-throat diffuser under investigation.

Before discussing second-throat diffusers, it is necessary to define what is meant by starting, operating, and minimum cell pressure ratios, which are the terms commonly used in describing the operation of ejector-diffuser systems (see Fig. 2). The starting pressure ratio $(p_{ex}/p_t)_{start}$, is the maximum exhaust pressure ratio at which minimum cell pressure ratio is obtained for decreasing values of p_{ex}/p_t. The operating pressure ratio is the maximum exhaust pressure ratio at which minimum cell pressure ratio can be maintained for increasing values of p_{ex}/p_t. The minimum cell pressure ratio is obtained for a given zero-secondary-flow, ejector-diffuser configuration when the cell pressure becomes independent of exhaust pressure. The starting pressure ratio is either equal to or less than the operating pressure ratio and is the pressure ratio which is most important in the design of an ejector system, whether the pressure ratio is controlled by varying the exhaust pressure or by varying the rocket chamber pressure. It should be noted, however, that minimum cell pressure ratio is affected by nozzle total pressure because of the Reynolds number effect, as previously reported in Ref. 4. Since the theoretical calculations of $(p_c/p_t)_{min}$ have been the subject of a previous investigation (Ref. 5), it will be assumed for the purposes of this report that a method similar to that discussed in Ref. 5 is available for calculating this pressure ratio.

SECTION II
DEVELOPMENT OF THEORY

The basic difference between the method developed in Ref. 2 for determining second-throat starting performance (which will be referred to herein as Method 1) and the improved method (Method 2) presented in this report is in the method for determining the conditions at station 2 (see Fig. 1). One of the most important requirements for calculating the ramp pressure drag and the resulting conditions at the second-throat

entrance is a knowledge of the driving nozzle free-jet flow field. The agreement of the experimental and theoretical Mach number distributions downstream of the nozzle exit in Ref. 5 indicated that the method of characteristics solution to the general isentropic flow equations provides a satisfactory method for determining the flow field approaching the second throat for the conical nozzles investigated to date. As the flow approaches the diffuser walls, it becomes nonuniform both axially and radically. The turning of such a flow field parallel to the diffuser walls can be treated approximately to determine the static pressure distribution along the walls, as suggested in Ref. 5, by considering small increments in the approaching flow to be uniform at some average Mach number and flow direction. The static pressure existing downstream of the oblique shock is then assumed to be constant along the associated Mach line as shown in Fig. 1. The Mach number preceding the ramp shock is determined from the calculated static pressures on the various Mach lines and the total pressure (which is assumed constant along the streamlines) downstream of the reflected boundary shock. A comparison of the experimental and theoretical pressures on the second-throat ramp in section 4.1 indicates that good agreement results with this method until the reflected free-jet boundary shock intersects with the ramp shock (Fig. 1). The deviation at this point is probably the result of neglecting the effects of boundary layer on the flow approaching the ramp and the assumption that the shock waves are not curved. An empirical assumption was therefore made to correct for this deviation by assuming that the pressure on the second-throat ramp is constant downstream of the shock intersection.

The general procedure which is followed in determining the conditions at the second-throat entrance (station 2) with Method 2 can be summarized as follows:

1. The minimum cell pressure ratio is obtained using a method similar to that discussed in Ref. 5. It is assumed that cell pressure is not affected by changes in diffuser geometry downstream of free-jet impingement.
2. The calculated cell pressure ratio is used with the method of characteristic solution for axisymmetric flow to determine the free-jet flow field approaching the second throat.
3. The ramp pressure and the conditions entering the throat are determined by assuming that the flow is turned through a two-dimensional shock system and that the ramp pressure is constant after the intersection of the reflected boundary shock and the ramp shock. The frictional forces, f_d and f_R,

the pressure drag force on the second-throat ramp, F_R, and the oblique shock location approaching the second-throat entrance are then determined.

4. The results are applied to the conservation equations to obtain the conditions entering the second throat at station 2, which are then used to determine the starting pressure ratio for a given second-throat configuration.

2.1 GENERAL EQUATIONS

This theoretical analysis is a continuation of that reported in Ref. 2 and utilizes the same general equations for determining second-throat performance, which were developed previously by applying the conservation equations between stations 1 and 2 and the following assumptions:

1. Flow is steady, adiabatic, and one-dimensional at stations 2 and 3,
2. Gas is perfect, and
3. Gas velocity in cell region is zero.

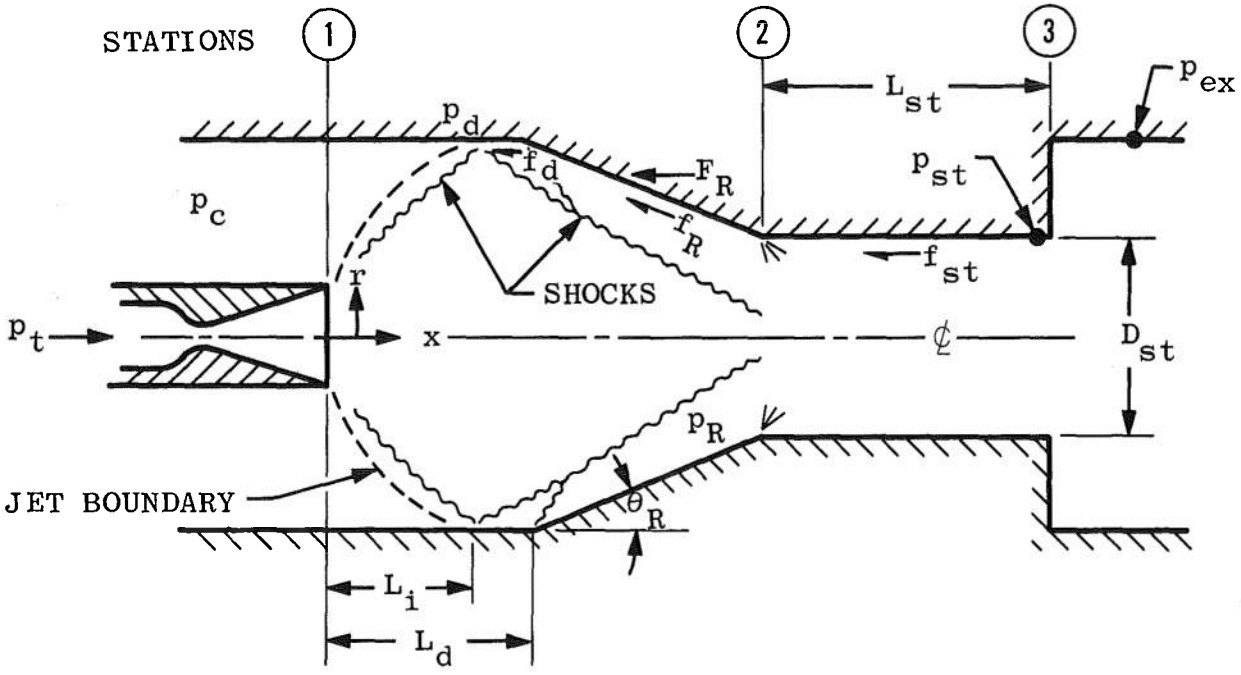

Thus, the axial force balance equation can be written

$$F_{i_x} - \underbrace{f_d - F_R - f_{R_x}}_{\text{drag forces}} = F_{2_x} \tag{1}$$

where

$$F_{i_x} = F_{ne_x} + p_c\,(A_d - A_{ne}) \tag{2}$$

$$f_d = \pi r_d \gamma \int_{L_i}^{L_d} C_f p_d M_d^2 \, dx \tag{3}$$

$$F_R = 2\pi \int_{r_{st}}^{r_d} p_R \, r \, dr \tag{4}$$

$$f_{R_x} = \frac{\pi}{2} \gamma \cot \theta_R \int_{r_{st}}^{r_d} C_f M_R^2 p_R \, r \, dr \tag{5}$$

$$F_{2_x} = 2\pi \int_{0}^{r_{st}} p_2 \, (1 + \gamma M_2^2) \, r \, dr \tag{6}$$

By assuming the flow to be one-dimensional at station 2, the conservation equations may be used to write

$$\frac{F_{2_x}}{\dot{m}\sqrt{R T_t}} = \frac{1 + \gamma M_2^2}{M_2 \sqrt{\gamma \left(1 + \frac{\gamma - 1}{2} M_2^2\right)}} \tag{7}$$

Once the variables which make up the left-hand side of this equation have been obtained, the Mach number may be obtained from the graphical solution shown in Fig. 3.

2.2 APPLICATION OF THEORY

The following sections indicate how the theoretical results up to this point may be applied to various second-throat configurations.

2.2.1 Application to Short Second Throats [$(L/D)_{st} < 1$]

The best method for obtaining the starting and operating pressure ratio for short second-throat diffusers is to use the predetermined supersonic Mach number at station 2 to determine the maximum pressure ratio, p_{st}/p_2, required to separate a turbulent boundary layer (see Fig. 1). This value is then used with the continuity equation

$$p_2/p_t = \frac{\dot{m}\sqrt{R T_t}}{p_t A_{st} M_2 \sqrt{\gamma \left(1 + \frac{\gamma - 1}{2} M_2^2\right)}} \tag{8}$$

to determine the overall starting pressure ratio, p_{st}/p_t. This method for determining short second-throat performance was developed in Ref. 2 by using the conservation equations and making the additional assumption that the frictional losses in the minimum area are negligible.

There is still some question as to which separation criteria should be used. For the semi-empirical method (Method 1) of determining second-throat performance developed in Ref. 2, Arens and Spiegler's separation pressure ratio (Ref. 3) gave good results. However, for the theoretical method developed in this report (Method 2), Mager's separation pressure ratio (Ref. 6) appeared to give better agreement with the

diffuser performance. The reason for the disagreement is unknown. A comparison of the separation pressure ratios obtained by these two methods is shown in Fig. 4 for $\gamma = 1.4$.

2.2.2 Application to Long Second Throats [$(L/D)_{st} > 5$]

The maximum diffuser exit pressure at which the long second-throat diffuser will start and operate can be determined by using the subsonic solution, M_3, of Eq. (7), together with the following additional assumptions for the flow between stations 2 and 3:

1. Frictional losses in the minimum area may be estimated by assuming a linear Mach number distribution from station 2 to 3 and a constant friction coefficient, and
2. The static pressure at station 3 equals the exhaust pressure, p_{ex}.

The starting and operating pressure can thus be obtained by calculating the subsonic exit Mach number, M_3, and using the previously calculated upstream Mach number, M_2, in Eq. (9), as developed in Ref. 2.

$$\frac{F_{2_x}}{\dot{m}\sqrt{R\,T_t}} = \sqrt{\frac{2\gamma}{\gamma-1}}\,\frac{C_f\,2\,(L/D)_{st}}{(M_3 - M_2)}\left[\sqrt{\frac{2}{\gamma-1} + M_3^2} - \sqrt{\frac{2}{\gamma-1} + M_2^2}\right] + \frac{1 + \gamma M_3^2}{M_3\sqrt{\gamma\left(1 + \frac{\gamma-1}{2}M_3^2\right)}} \tag{9}$$

A graphical solution for M_3 is presented in Fig. 3a for $\gamma = 1.4$, $(L/D)_{st} = 8$, and $C_f = 0.003$. The value of M_3 is then used in the continuity equation to calculate the maximum starting and operating diffuser exit pressure ratio.

$$\frac{p_{st}}{p_t} = \frac{\dot{m}\sqrt{R\,T_t}}{p_t A_{st} M_3\sqrt{\gamma\left(1 + \frac{\gamma-1}{2}M_3^2\right)}} \tag{10}$$

2.2.3 Applications to Intermediate Length Second Throats [$1 < (L/D) < 5$]

An experimental investigation of intermediate length second-throat performance indicated that the linear interpolation between the short and long second-throat theories suggested in Ref. 2 gave the best results. The experimental second-throat performance using conical nozzles (Ref. 2) and cylindrical diffuser performance using annular nozzles (Ref. 7) both indicate that this interpolation can be made between $(L/D)_{st} = 0.5$ and 5.0.

An empirical mathematical flow model was also developed for predicting the performance of intermediate length second throats. Although this model gave good results, it is not a physically realistic flow model. The development of this mathematical model and its results are included in Appendix I.

2.2.4 Application to Second Throats with Centerbodies

The theoretical analysis of second-throat diffusers with centerbodies uses the preceding theory with the following additional assumptions:

1. The pressure on the centerbody cone is calculated using conical flow relations, and
2. The Mach number approaching the supporting vanes is subsonic just prior to unstarting the ejector.

It should also be noted that this method has a limited application in short, second-throat configurations. The centerbody must be positioned such that the centerbody shock impinges upstream of the throat (see section 4.2.4).

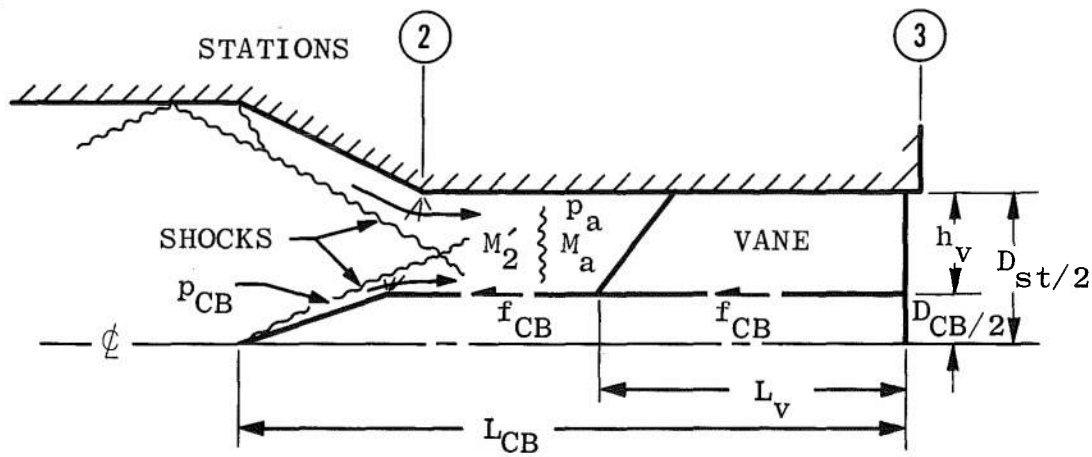

The force at station 3 can be written as

$$F_{3_x} = F_{2_x} - f_{CB} - \pi \int_0^{r_{CB}} p_{CB}\, r_{CB}\, dr_{CB} \tag{11}$$

where $F2_x$ is determined from Eq. (7).

For centerbodies without supporting vanes in the throat

$$f_{CB} = \frac{C_f}{2} \gamma\, p_a\, M_a^2\, \pi\, (D_{st} - D_{CB})\, L_{CB} \tag{12}$$

and for those using supporting vanes in the throat

$$f_{CB} = \frac{C_f}{2} \gamma\, p_a\, M_a^2 \left[\pi\, (D_{st} - D_{CB})\, L_{CB} + 2N\, (h_v)\, L_v\right] \tag{13}$$

where $C_f = 0.003$ and M_a and P_a are determined from the normal shock relations for the Mach number, M_2', which is calculated for the conditions entering the throat. This Mach number, M_2', in front of the normal shock is assumed to be an average of the supersonic Mach numbers downstream of the ramp and centerbody shocks at station 2. Equation (11) can be further written as

$$\frac{F_{3_x}}{\dot{m}\sqrt{R T_t}} = \frac{1 + \gamma M^2}{M\sqrt{\gamma\left(1 + \frac{\gamma - 1}{2} M^2\right)}} \tag{14}$$

where M is either supersonic or subsonic, depending on whether a short or long second throat is being considered. The starting pressure ratio is then calculated using the previously discussed equations (Eqs. (8) or (10)) for either a short or long second throat.

Figure 5 shows that the pressure force on the second-throat ramp as well as the conditions entering the second throat are affected at certain locations of the centerbody. Comparisons of theoretical and experimental starting pressure ratios for the configurations investigated in section 4.2.4 indicate that this effect can be neglected providing deviations less than 10 percent are not required.

SECTION III
EXPERIMENTAL INVESTIGATION

The experimental investigation of second-throat diffuser performance discussed in this report is a continuation of the study reported in Ref. 2. Additional experimental results are presented in support of the following theoretical investigations:

1. Wall static pressure distribution on the second-throat ramp and flow conditions entering the throat,
2. Development of a mathematical flow model to predict intermediate length second-throat performance,
3. Effects of centerbody position on second-throat performance, and
4. Second-throat performance using annular and cluster nozzles.

3.1 EXPERIMENTAL APPARATUS

Eight nozzles and eight second-throat diffusers (Table I) were tested in various combinations during this phase of the investigation of the 55 configurations listed in Table II.

3.1.1 Test Hardware Description

The nozzles were concentrically located in a cylindrical diffuser with the upstream end of the diffuser attached to a sealed plenum. A typical test configuration is shown in Fig. 6. The nozzles were mounted on a movable section of inlet supply pipe which permitted the nozzle to be translated approximately 9.0 in. along the horizontal centerline of the diffuser system. The design of the "O" ring seals in the telescoping sections permitted the nozzle to be positioned during a test without leakage into the cell region. The position of the nozzle with respect to the second throat was indicated by a calibrated counter, which registered the rotations of the actuating mechanism.

The nozzle configurations which were tested are illustrated in Fig. 7, and the diffuser configurations are shown in Fig. 8. The code designation for the various combinations of these configurations is included in Table I. A typical ejector configuration designation would be 4-5d-CB, which indicates an 18-deg conical nozzle with an area ratio of 25.0 exhausting into a 10.19-in.-diam cylindrical diffuser with a second-throat diffuser having a throat length to diameter ratio, $(L/D)_{St}$ = 8.1, an effective contraction ratio, $(A_{St}-A_{CB})/Ad$ = 0.417, and an 18-deg centerbody located in the throat.

3.1.2 Instrumentation

The parameters measured during this investigation were: cell pressure, p_C; static pressures along the second throat and cylindrical diffuser walls, p_W; static pressures on the second-throat ramp, p_R; nozzle total pressure, p_t; nozzle total temperature, T_t; and second-throat diffuser exit static and total pressures, p_{St} and p_{t_r}. Table III contains the range of the measured parameters and the type of measuring instrument used for each.

3.2 EXPERIMENTAL PROCEDURE

Prior to each test, the nozzle, test cell, and instrumentation lines were pressure checked to minimize the possibility of leakage. A vacuum check was also made prior to each test to reduce the possibility of instrumentation leakage. Inlet air was supplied from the RTF compressors at a pressure, p_t, as high as 46 psia and at a temperature of approximately 80°F. The ejectors exhausted into the RTF exhaust machines, which provided pressures as low as 7 mm HgA. An electrically operated throttling valve in the exhaust ducting was used to control the exhaust pressure. The inlet supply pressure was manually controlled by a gate-type valve.

The maximum second-throat diffuser exit pressure, $(p_{st})_{start}$, at which the ejector became started was obtained for each configuration at a given second-throat and/or centerbody position and total pressure, p_t, by decreasing the exhaust pressure until the cell pressure, p_c, reached a minimum value. The exhaust pressure was then increased until the ejector again became unstarted (where p_c started to increase) to determine the maximum operating diffuser exit pressure. This procedure was repeated at various nozzle positions to determine the effect of second-throat location on ejector second-throat diffuser performance. The wall pressures on the second-throat diffuser were recorded when the cell pressure was at the minimum value. During the centerbody investigation, the above procedures were repeated at various nozzle positions and centerbody positions to determine the effects of centerbody position on second-throat performance. The second-throat exit total pressure, p_{t_r}, surveys made during the intermediate length second-throat flow-model investigation were recorded just prior to unstarting the ejector.

SECTION IV
DISCUSSION OF RESULTS

During the previous second-throat diffuser investigation in Ref. 2, the empirical method for predicting the pressure force on the second-throat ramp gave good results for conical nozzles with uniform exit Mach numbers. However, the results shown in Table II for annular nozzles indicate that this method is not adequate for predicting the starting pressure ratio of ejector systems which have highly nonuniform Mach number distribution at the nozzle exit. Typical nonuniform nozzle exit Mach number distributions are shown in Fig. 9. Even the flow from nozzles with uniform exit flow becomes slightly nonuniform as it approaches the second throat (Fig. 10). A more accurate procedure for predicting the pressures on the second-throat ramp and the conditions approaching the throat entrance (as discussed in section II) was therefore developed. Comparisons of experimental and theoretical results show that this procedure is a prerequisite to the theoretical calculation of the starting pressure ratio for second-throat diffusers whose approaching flow field is highly nonuniform.

4.1 RAMP PRESSURE FORCE

Figures 11a through f show a comparison of the experimental and theoretical ramp pressure distribution. It will be noted that in each case, the theoretical pressure distribution is less than the experimental

value after the intersection of the impingement shock and the ramp shock. There are several things which may account for this. One is the presence of boundary layer, which was neglected, and another is the assumption that the impingement shock originates where the inviscid jet boundary strikes the cylindrical diffuser rather than at the impingement of the stagnating streamline as shown by the following sketch. However, this deviation is more than likely the result of the two-dimensional flow

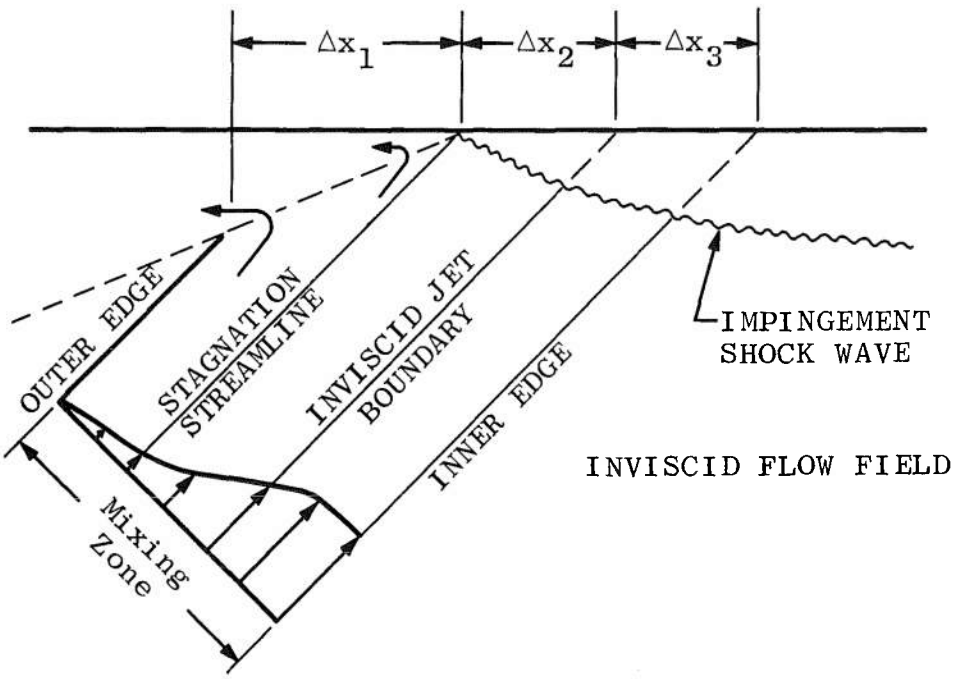

Idealized Flow Phenomena

assumption, which becomes inadequate as the relations across the oblique shocks are analyzed at greater distances downstream of the free-jet impingement. The best results for predicting the pressure force acting on the ramp were obtained by integrating the pressure forces along the ramp and assuming the pressure after the shock intersection to be constant. Comparisons of the experimental and theoretical ramp pressure forces using this procedure showed an agreement within approximately five percent for the conical nozzle configurations investigated. This results in an approximate 1.7-percent deviation in the overall starting pressure ratio.

A theoretical Method 2 calculation of the ramp pressures using annular and cluster nozzles was not made because of the unavailability of a flow field. However, the experimental ramp pressures are shown in Figs. 12a through c.

Centerbody position will affect the pressures on the ramp as is shown in Fig. 5; however, a theoretical method for calculating this effect was not included in this investigation. Neglecting the effect of centerbody position in the theoretical calculations is reflected in the percent deviation shown in Table II. A comparison of the force on the ramp for a centerbody located at position (1) (Fig. 5) shows that the force on the ramp is increased approximately two and one-half times that observed when the centerbody is retracted to position (5) (Fig. 5). This would result in approximately a 20-percent deviation in the overall theoretical starting pressure ratio and would indicate that the effect of centerbody position should be considered for an accurate calculation. However, later comparisons of the experimental and theoretical starting pressure ratios (neglecting the effect of the centerbody on ramp pressure) show that the actual deviation was much less.

4.2 COMPARISON OF EXPERIMENTAL AND THEORETICAL SECOND-THROAT PERFORMANCE

Method 1, as presented in Ref. 2, resulted in a satisfactory procedure for calculating the starting pressure ratio for second-throat ejector-diffuser systems with uniform nozzle exit flow. Although Method 2 gives as good or better results than Method 1 for these same systems (see Table II), Method 2 was developed for the primary purpose of arriving at a more general procedure for calculating the performance of systems whose nozzle exit flow is nonuniform. Unfortunately, the nonuniform flow fields for the annular nozzles tested were not available to make a comparison of the improved theory and the experimental data. However, the good agreement of the experimental data with the results from Method 2 for the conical and contour nozzles, whose flow fields were available, should indicate that Method 2 will be satisfactory once the free-jet flow field is determined. This will be verified pending further development of a method to calculate the annular nozzle flow fields.

The theoretical starting pressure ratio for the annular nozzles listed in Table II was calculated by using Method 1 and assuming an average nozzle exit Mach number (see Fig. 9). However, these results are not discussed in detail since Method 1 does not provide an accurate method for calculating the ramp force and the conditions approaching the throat for these nozzles.

4.2.1 Short Second Throats [$(L/D)_{st} < 1$]

Comparison of the experimental and theoretical starting pressure ratios for six short second-throat configurations listed in Table II

resulted in a maximum deviation from the experimental results of 2.9 percent using Method 2 (see Fig. 13). The new theoretical method predicted the starting performance more accurately for all short second-throat configurations investigated.

4.2.2 Long Second Throats [$(L/D)_{st} > 5$]

The theoretical starting and operating pressure ratio was determined for two long second-throat configurations, (3-5d and 4-5d) using Method 2. Comparisons with the experimental results showed a maximum deviation of 6.8 percent for conical nozzles and 2.2 percent for the one contour nozzle investigated using Method 2. Method 1 resulted in a maximum deviation of 9.7 percent for conical nozzles and 11.7 percent for the contour nozzle. Method 2 gives better results for the contour nozzle because it takes into account the nonuniform flow condition approaching the second throat shown in Fig. 10.

4.2.3 Intermediote Length Second Throots [$1 < (L/D)_{st} < 5$]

The starting pressure ratio of intermediate length second throats can be determined within approximately 10 percent by taking a linear interpolation between the short throat theoretical results at $(L/D)_{st} = 0.5$ and the long second-throat theoretical results at $(L/D)_{st} = 5.0$ (see Fig. 14). A more theoretical approach to determining the performance of intermediate length second throats was attempted, but a satisfactory procedure did not develop. The mathematical flow model which was developed gave accuracies equal to the linear interpolation; however, the flow model is questionable. Comparisons of the experimental data with the theoretical results for this mathematical flow model are given in Appendix I.

4.2.4 Centerbody Second Throots

The performance of two centerbody second-throat configurations (Fig. 8) was investigated - one in a short second throat without supporting vanes in the minimum area section and one in a long second throat with supporting vanes in the throat. A comparison of the theoretical and experimental starting pressure ratios for the short second-throat configurations investigated shows that a maximum deviation of 10.9 percent was obtained until the shock generated from the centerbody impinged on the throat, as shown by point (a) in Fig. 15a. The large deviation which exists downstream of point (a) is believed to be the result of the centerbody shock on the second-throat separation characteristics. The theoretical results upstream of point (a) were obtained using the procedures outlined in Method 2. However, as was mentioned in section 4.1, the effect of the centerbody on second-throat ramp pressure drag was not

considered. Figure 15a further indicates that the centerbody configurations tested gave the best performance (maximum starting pressure ratio) when the centerbody was positioned such that the shock was impinging upon the ramp. This is not to be considered as being generally true since it depends upon the geometry of the second throat (contraction, throat length, etc.). When the second-throat contraction is near its limit, the forces on the ramp should be kept to a minimum.

Figure 15b shows that for configuration 3-5d-CB the addition of a centerbody required a decrease in p_{st}/p_t to start the ejector system. An analysis of the losses within the system indicated that this was due to the large frictional losses caused by the supporting vanes in the minimum area section. A comparison of the theoretical and experimental starting pressure ratios showed a maximum deviation of 10.5 percent. Figure 15b shows that there is a centerbody position where the ejector would not restart. However, the theoretical calculations of the starting performance for the centerbody in that position indicated that the starting characteristics of the ejector were near the starting limit.

4.2.5 Cluster Nozzle Configurations

The second-throat performance with annular nozzles, which has been discussed in the preceding section, clearly indicates that a procedure similar to the proposed method (Method 2) is necessary to predict accurately the starting pressure ratio. Cluster nozzle configurations are similar in that they, too, have nonuniform flow conditions at the nozzle exit. An attempt to determine theoretically by Method 1 the flow conditions approaching the second throat for a four-nozzle cluster configuration shown in Fig. 7 was made by using the experimental cell pressure ratio, an experimental average ramp pressure, and assuming the diffuser diameter to be $D_d' = 4.301$ in. Table II indicates that a maximum deviation of 29 percent results. This is the result of using an empirical procedure for calculating the conditions entering the second throat. Unfortunately, an adequate flow field was not available to calculate theoretically the performance using Method 2.

SECTION V
APPLICATION TO DESIGN OF SECOND-THROAT DIFFUSER SYSTEMS

The application of the basic theory to given second-throat diffuser designs has been the primary objective in the preceding sections. However, the person who has the problem of designing an ejector-diffuser system to successfully test a given rocket motor at a specified altitude condition must approach the theory from a different aspect. It is,

therefore, desirable to specify the procedures which should be followed to use effectively the theories in the design of a second-throat diffuser. The procedures presented here are general, such that they can be applied to any of the configurations discussed.

It is first assumed that the following information is given:

1. Rocket motor nozzle geometry,
2. Ratio of specific heats,
3. Altitude pressure desired,
4. Rocket chamber pressure,
5. Available minimum diffuser exhaust pressure, and
6. Available maximum diffuser system length and diameter.

There are several ways one may approach the problem depending upon the test objective. However, for the purpose of discussion, it is assumed that the main purpose of the test is to ignite the rocket motor and record the steady-state thrust at a given altitude.

The initial altitude condition prior to firing is obtained using a steam ejector downstream of the nozzle. The details of the design of the steam ejector are not discussed because they are similar to the design of a hot rocket exhaust gas ejector system. It should be noted, however, that the objective requires that the steam ejector obtain a cell pressure equal to that which the hot rocket exhaust gas ejector system will obtain. If a centerbody-type steam ejector is used, it may be desirable to locate the centerbody as close to the nozzle exit as possible to minimize the recirculation of hot exhaust gases and variations in cell pressure during the tailoff transient (during rocket shutdown). However, the influence of centerbody position on second-throat performance (as well as centerbody heat transfer problems) must be taken into account. The configuration must be analyzed closely to ensure that the position of the centerbody will not interfere with starting of the ejector.

The first parameter to determine is the capture diffuser diameter required to obtain the test altitude. This can be found by an iteration procedure using the theory discussed in Ref. 5, which has been programmed on a 7074 computer. The flow field downstream of the nozzle and the free-jet impingement point of the stagnating streamline on the capture duct can then be determined by using the techniques discussed in Ref. 5. The second-throat ramp should be located just downstream of the free-jet impingement point on the cylindrical diffuser (see Ref. 2). The optimum second-throat ramp angle, which should be selected, will depend on the approaching flow conditions; however, Ref. 1 indicated

that the starting pressure ratio was rather insensitive to ramp angle for the conical nozzles investigated. (Ramp angle was varied from 6 to 18 deg.)

The next step would be to determine the pressure on the second-throat ramp. To accomplish this, the steps outlined in the beginning of section II are required. The maximum second-throat contraction can, therefore, be approximated by assuming $M_2 = 1.0$ and solving for F_{2_x} in Eq. (7). The second-throat contraction can then be calculated using Eq. (1) and neglecting the frictional forces for the first approximation. If a centerbody is employed in the second throat, then several iterations are required to determine the values of M_a and P_a in Eq. (12) or (13) since the centerbody frictional forces may become appreciable. Also, the design contraction ratio, A_{st}/A_d, should have at least a 10-percent margin of safety greater than the limiting contraction ratio to ensure that the ejector will start. Once the design contraction is determined, the length of the minimum area section should be made as long as possible (up to approximately five throat diameters). This analysis also assumes no subsonic diffuser is used. The maximum starting pressure can then be calculated using one of the applicable equations given in the preceding sections. Should the calculated starting pressure ratio be less than the available starting pressure ratio, it may be necessary to reduce the capture diffuser diameter and compromise the altitude requirements to obtain a system which will operate at the available pressures.

SECTION VI
CONCLUSIONS

Based on the results of this investigation, it can be concluded that an accurate theoretical method has been developed for analyzing the starting characteristics of a given second-throat, ejector-diffuser system subject to the following limitations:

1. The location of the free-jet impingement of the stagnating streamline must be determined,
2. The flow field approaching the second throat must be known, and
3. For short second-throat diffusers with centerbodies, the shock generated by the centerbody must impinge upstream of the minimum area section.

Further work which should be accomplished to understand more fully some of the observed experimental trends includes

1. The development of a computer program for determining the flow field approaching and entering the minimum area section of a second throat which could be applied to nozzles whose exit flow field is nonuniform, and
2. A study to determine the internal flow separation phenomena which take place in intermediate length second throats and in short second throats with a centerbody positioned such that the generated shock impinges in the throat.

REFERENCES

1. Bauer, R. C. and German, R. C. "The Effect of Second-Throat Geometry on the Performance of Ejectors without Induced Flow." AEDC-TN-61-133 (AD267263), November 1961.
2. Panesci, J. H. and German, R. C. "An Analysis of Second-Throat Diffuser Performance for Zero-Secondary-Flow Ejector Systems." AEDC-TDR-63-249 (AD426336), December 1963.
3. Arens, M. and Spiegler, E. "Shock-Induced Boundary Layer Separation in Overexpanded Conical Exhaust Nozzles." AIAA Journal, Vol. 1, pp. 578-581, March 1963.
4. Bauer, R. C. and German, R. C. "Some Reynolds Number Effects on the Performance of Ejectors without Induced Flow." AEDC-TN-61-87 (AD262734), August 1961.
5. Bauer, R. C. "Theoretical Base Pressure Analysis of Axisymmetric Ejectors without Induced Flow." AEDC-TDR-64-3 (AD428533), January 1964.
6. Mager, A. "On the Model of the Free, Shock-Separated, Turbulent Boundary Layer. "Journal of the Aeronautical Sciences, Vol. 23, No. 2, pp. 181-184, February 1956.
7. German, R. C., Panesci, J. H., and Clark, H. K. "Zero Secondary Flow Ejector-Diffuser Performance Using Annular Nozzles." AEDC-TDR-62-196 (AD294138), January 1963.

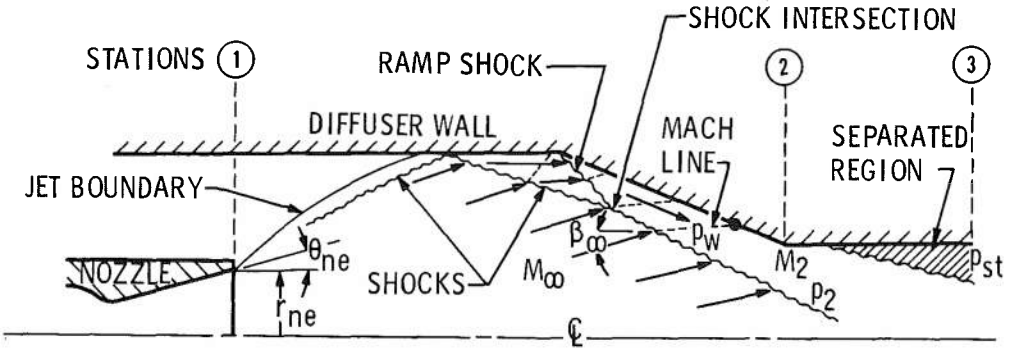

Fig. 1 Typical Flow Model for Second-Throat Operation Just Prior to Unstart Using a Conical Nozzle

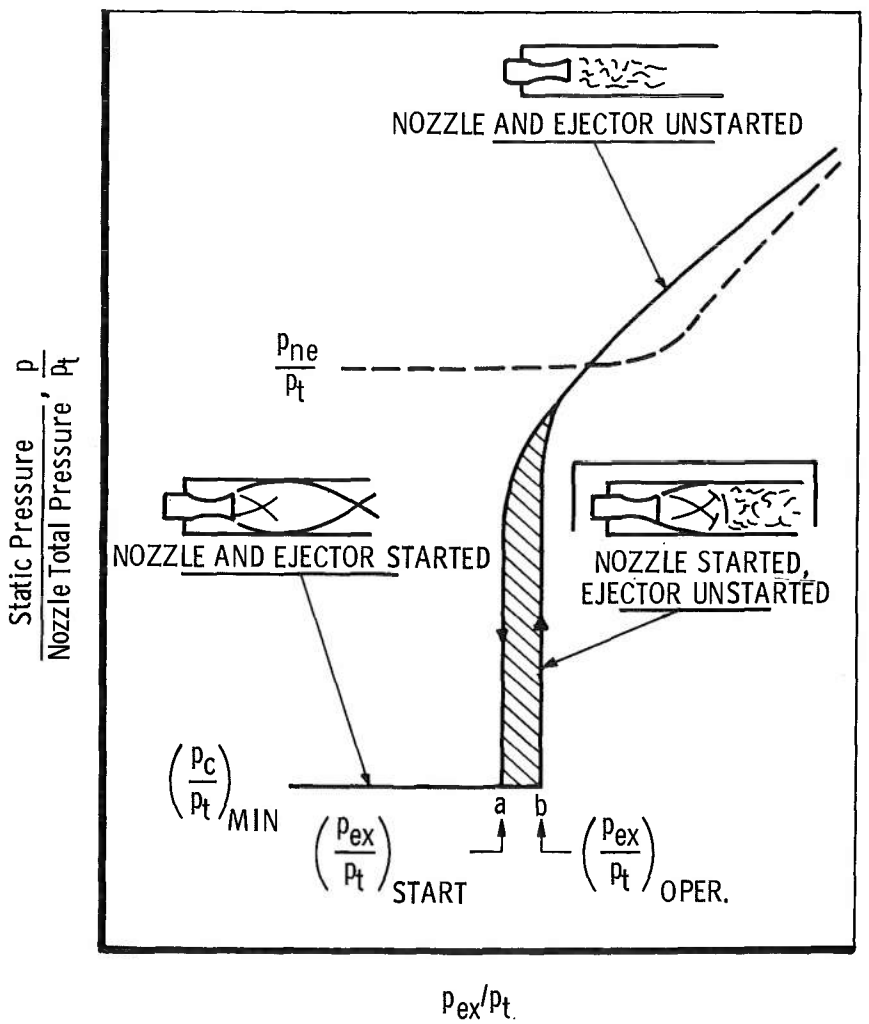

Fig. 2 Typical Ejector System Starting Phenomena for Constant Nozzle Total Pressure

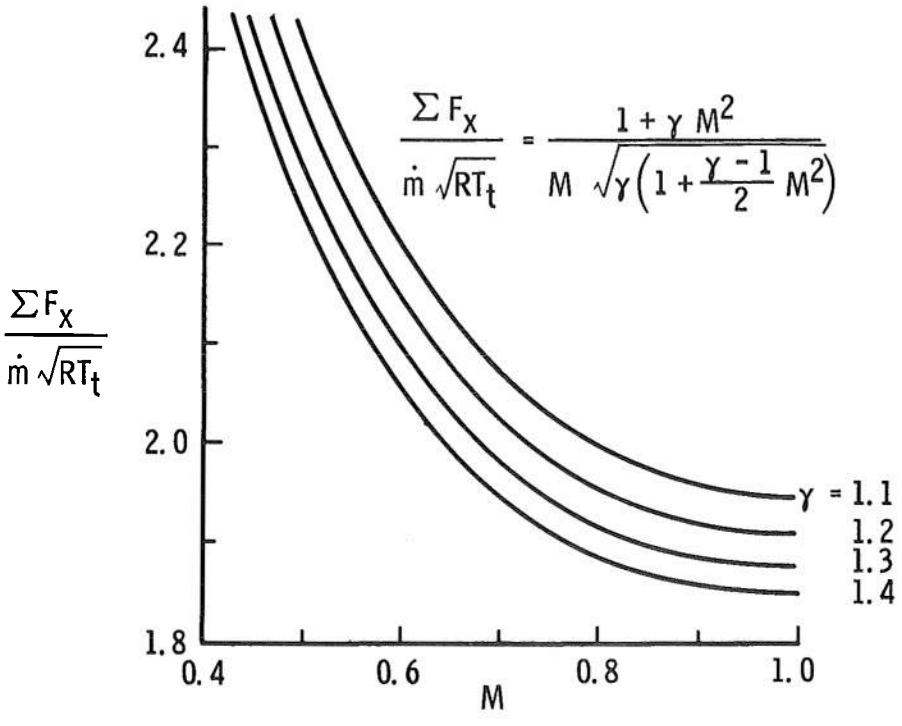

a. Subsonic Solution

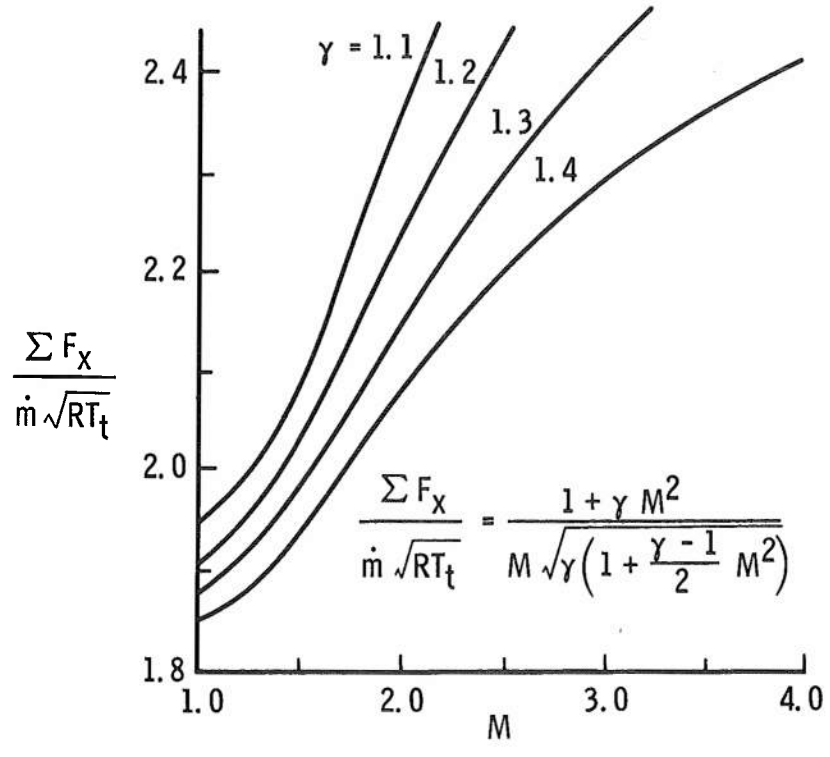

b. Supersonic Solution

Fig. 3 Graphical Solution for Mach Number

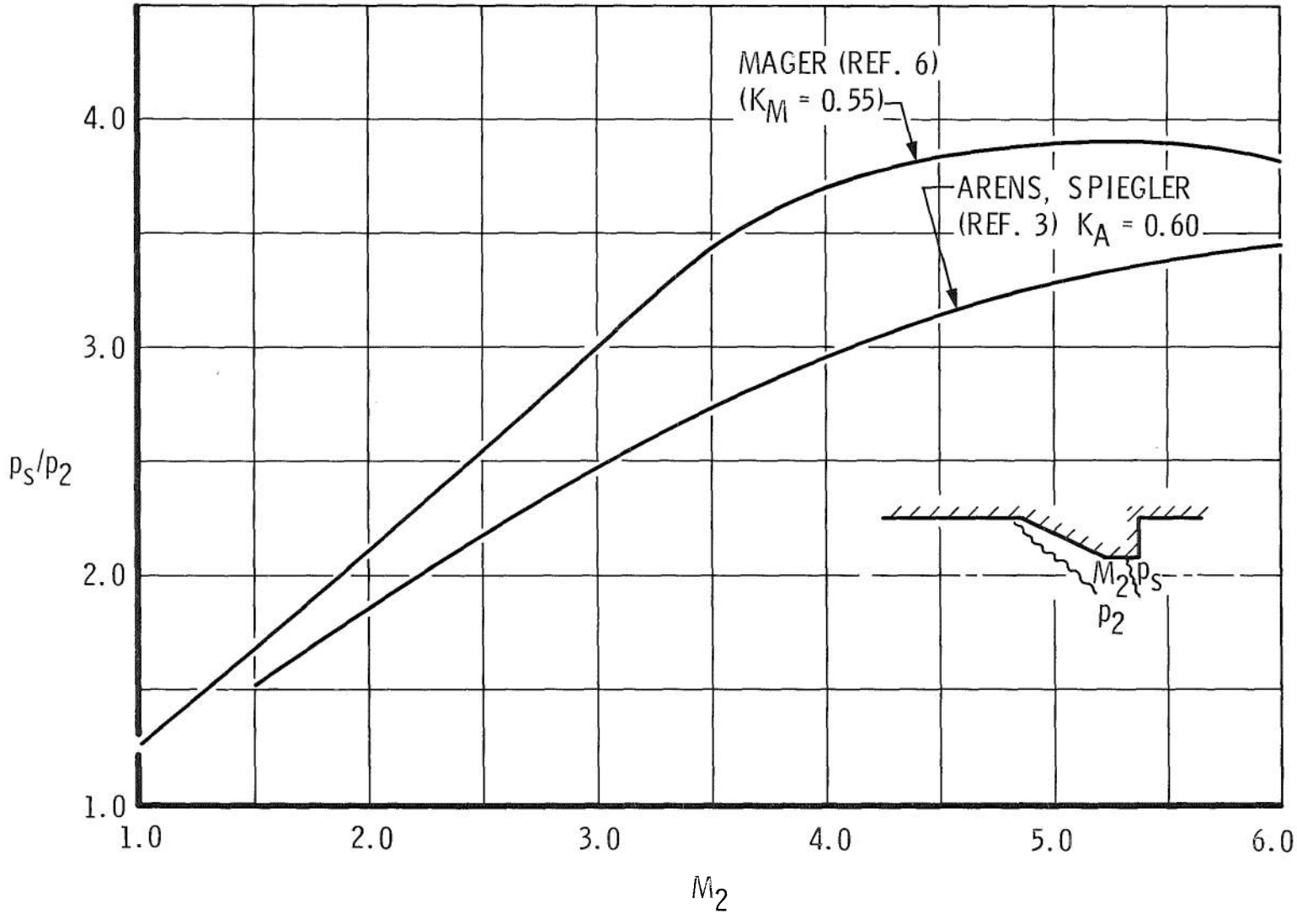

Fig. 4 Methods for Determining Free, Shock-Separation Pressure Ratio

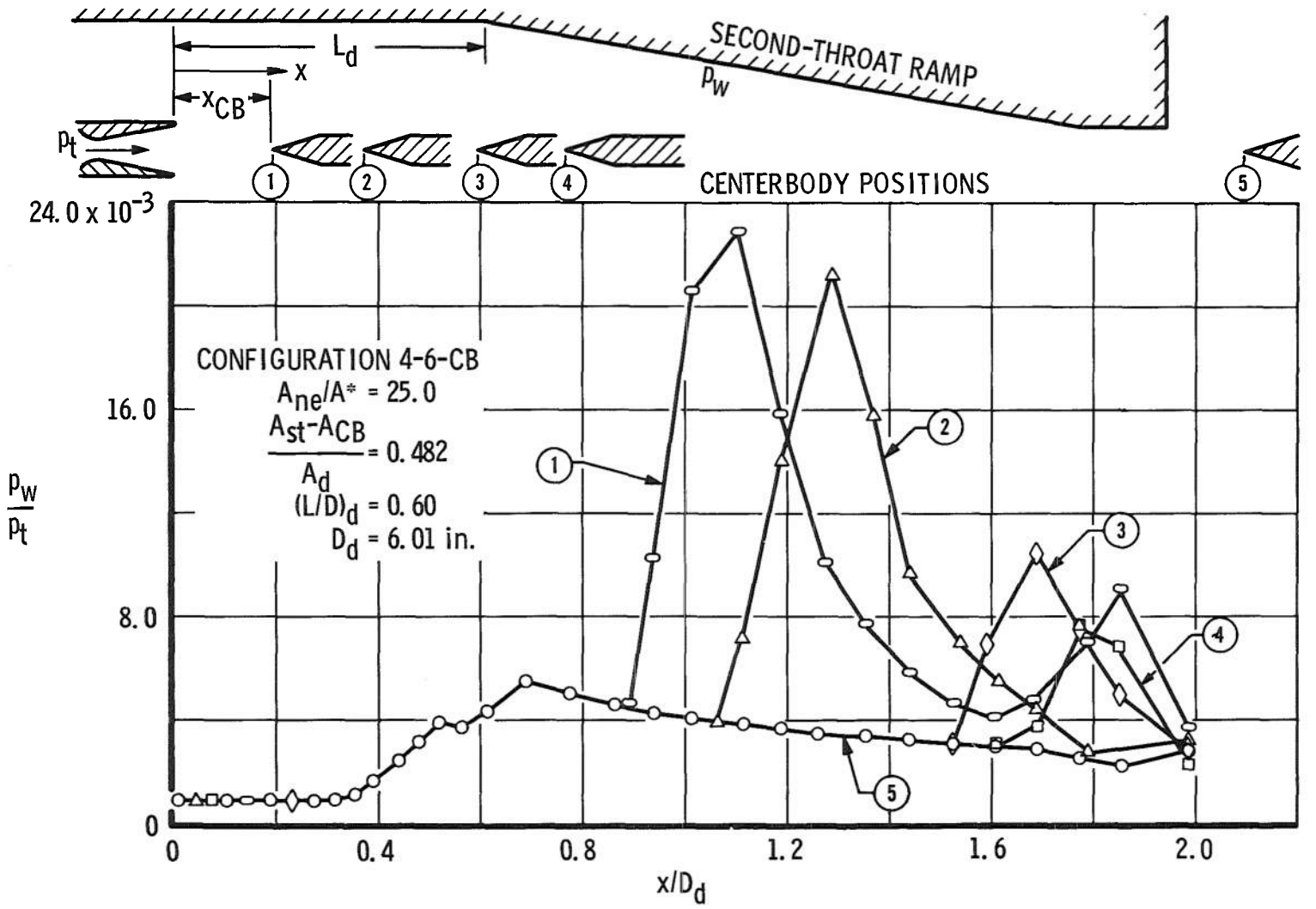

Fig. 5 Effect of Centerbody Location on Second-Throat Ramp Pressure

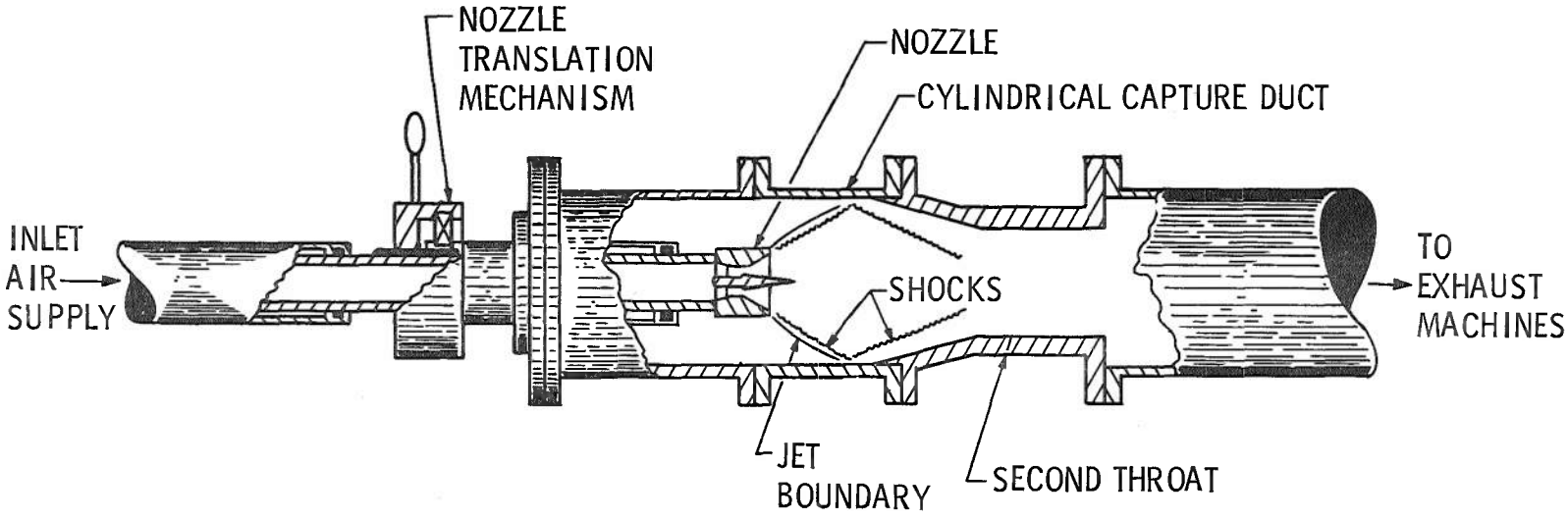

Fig. 6 Typical Ejector-Diffuser Configuration

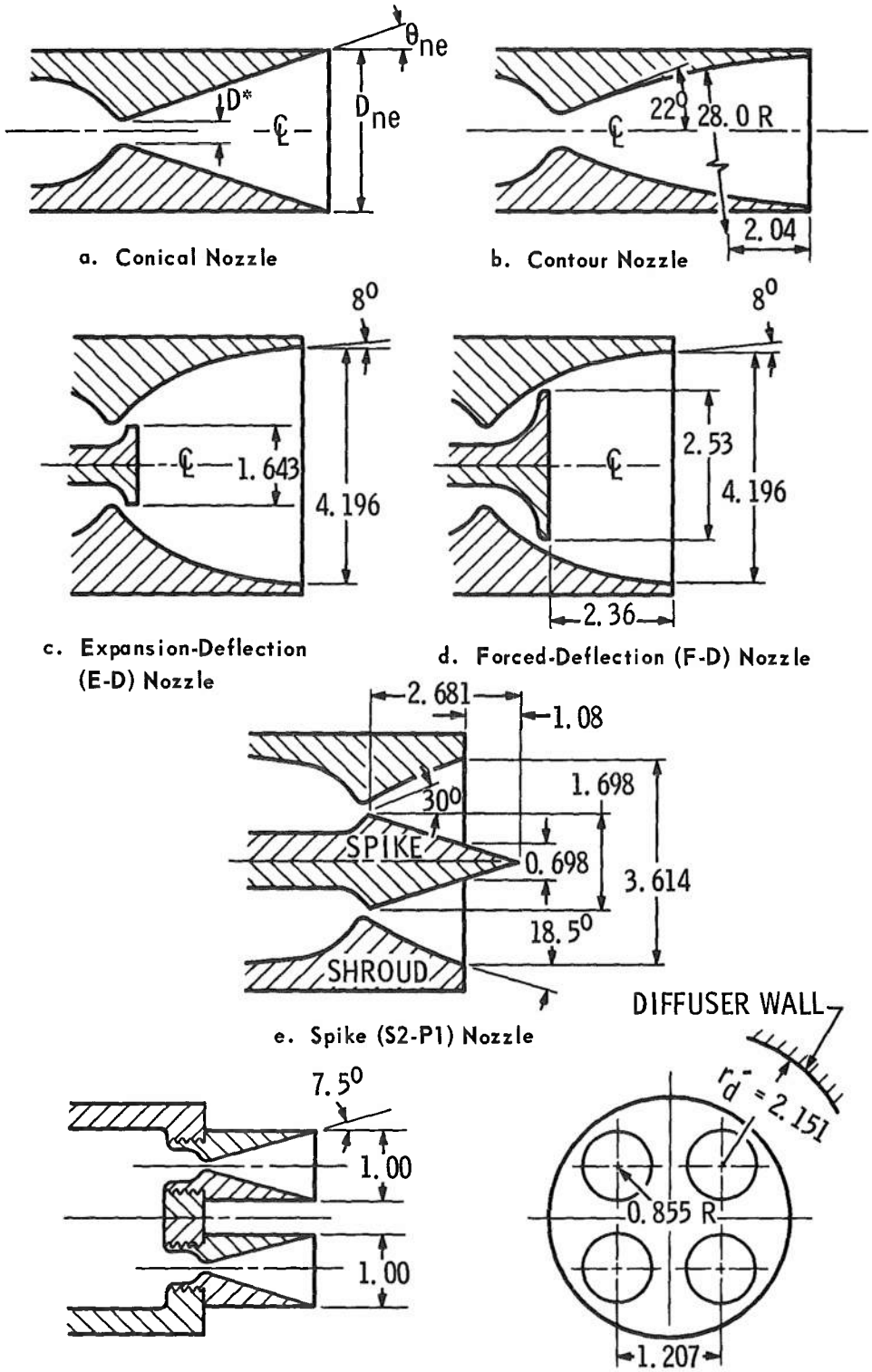

a. Conical Nozzle

b. Contour Nozzle

c. Expansion-Deflection (E-D) Nozzle

d. Forced-Deflection (F-D) Nozzle

e. Spike (S2-P1) Nozzle

f. Four-Nozzle Cluster

Fig. 7 Nozzle Configurations Investigated

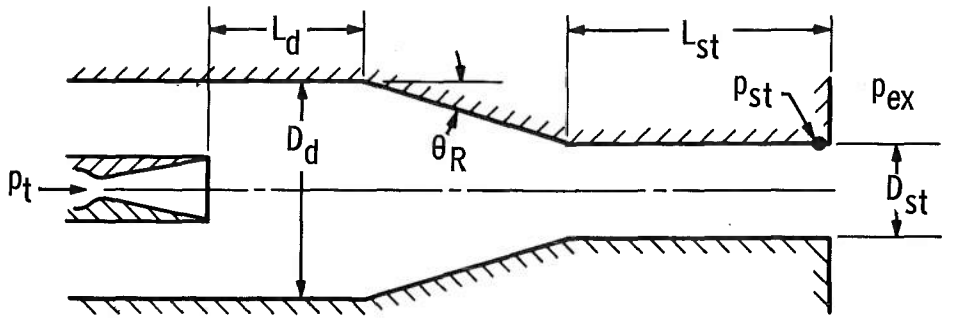

a. Typical Short, Intermediate, and Long Second-Throat Test Configuration

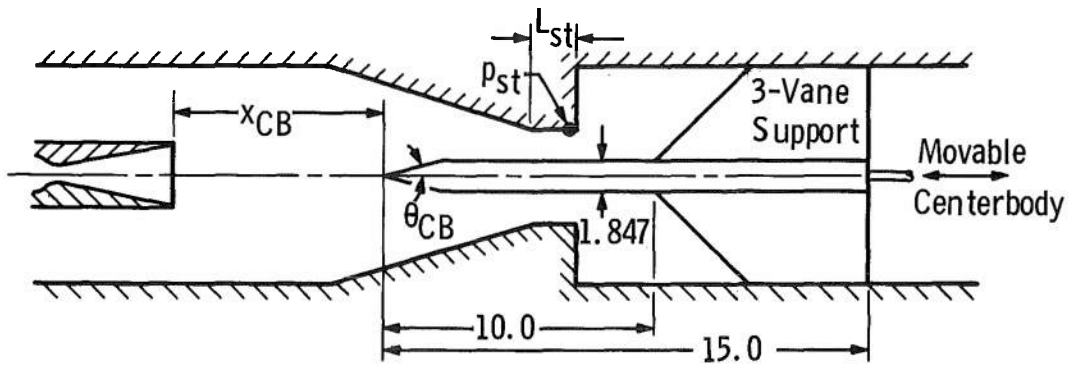

b. Centerbody Test Configuration (D_d = 6.01 in.)

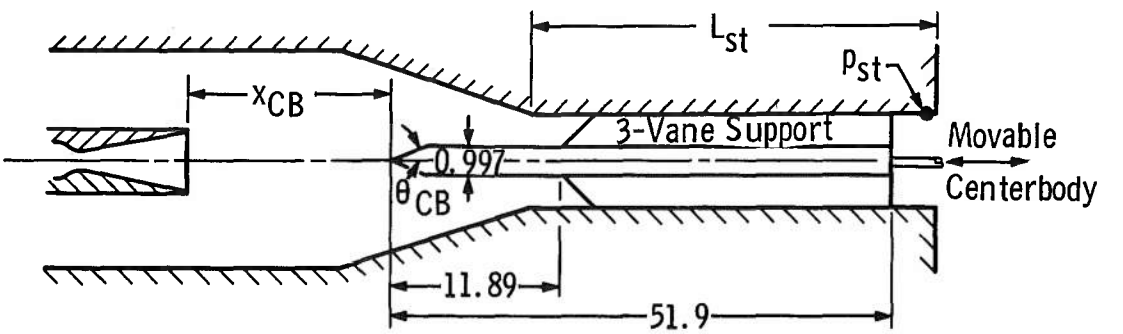

c. Centerbody Test Configuration (D_d = 10.19 in.)

Fig. 8 Second-Throat Diffuser Configurations Investigated

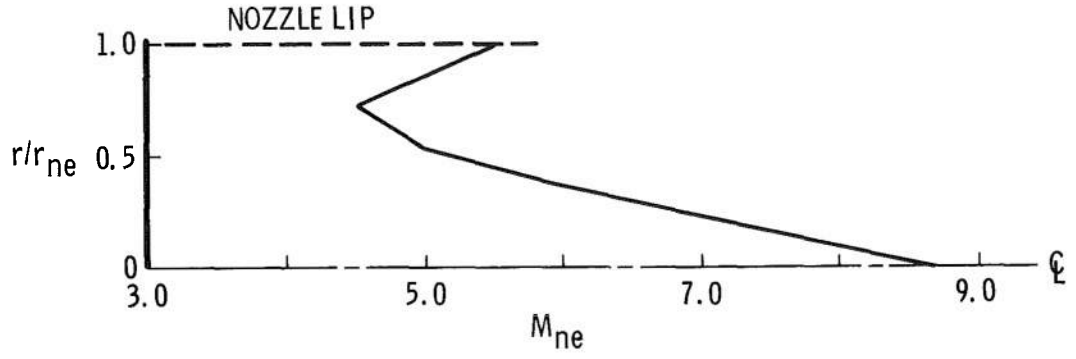

a. Expansion-Deflection Nozzle (E-D)

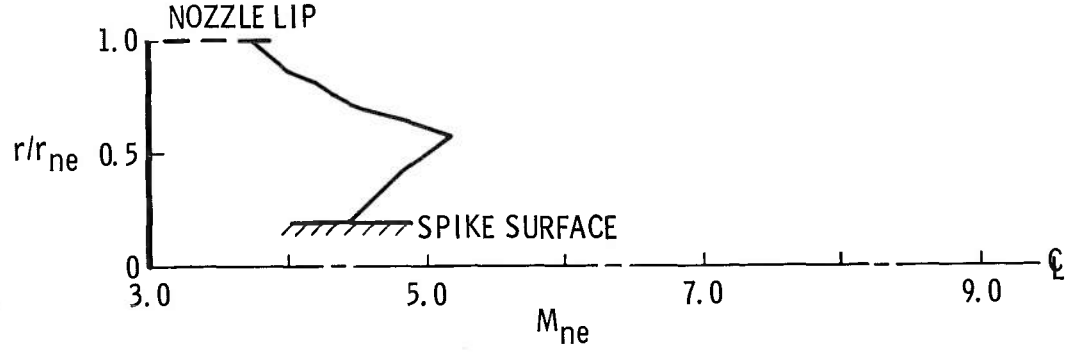

b. Annular Spike Nozzle (S2-P1)

Fig. 9 Nozzle Exit Mach Number Distribution for Annular Nozzles

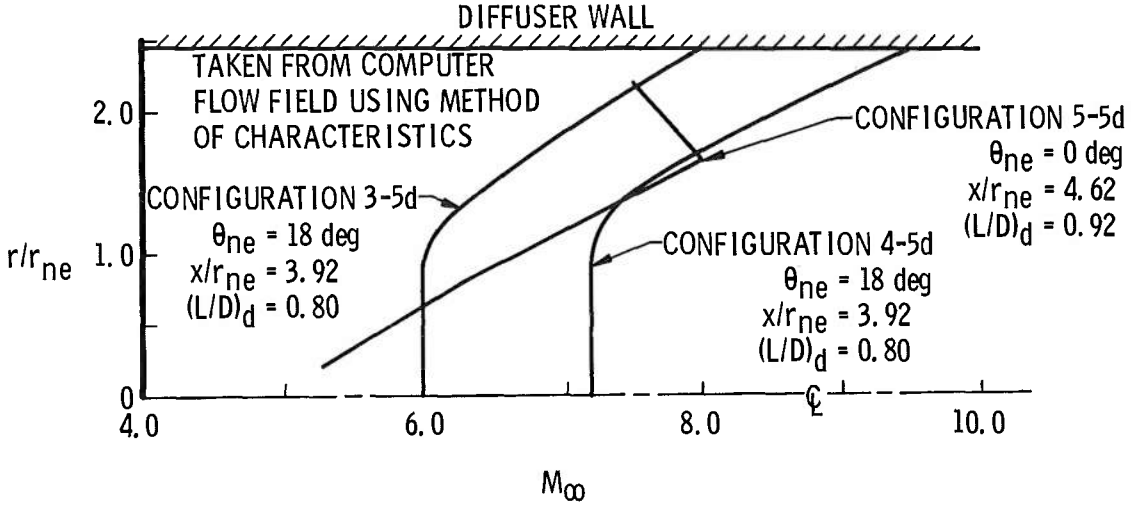

Fig. 10 Mach Number Distribution at Second-Throat Ramp Lip Station

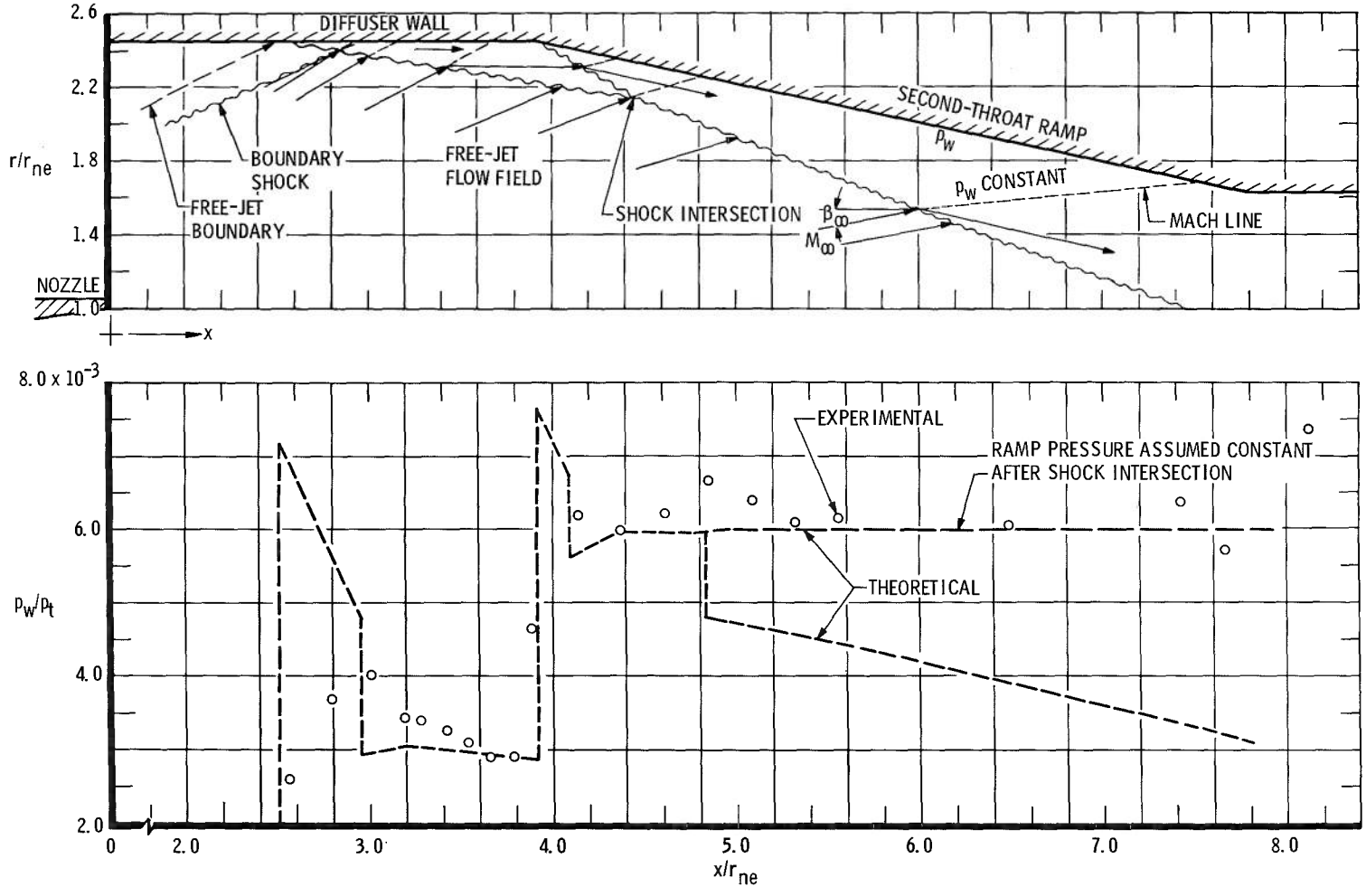

a. Configuration 3-5d, $(L/D)_d = 0.80$

Fig. 11 Experimental and Theoretical Static Pressure Distributions on Second-Throat Ramp (for Minimum P_{ex}/P_t)

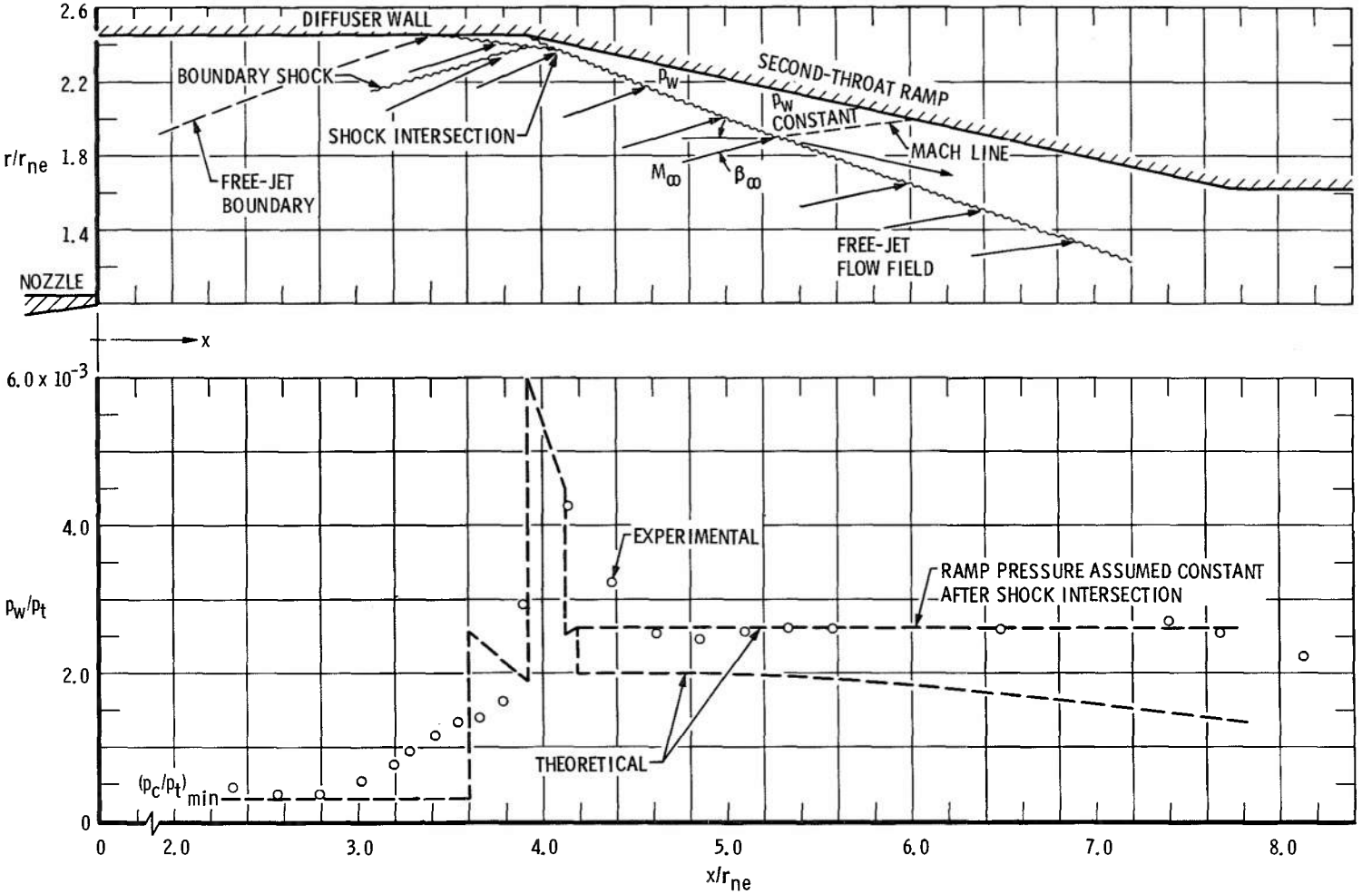

b. Configurations 4-5a,-5b,-5c,-5d, and-5e, $(L/D)_d$ = 0.80

Fig. 11 Continued

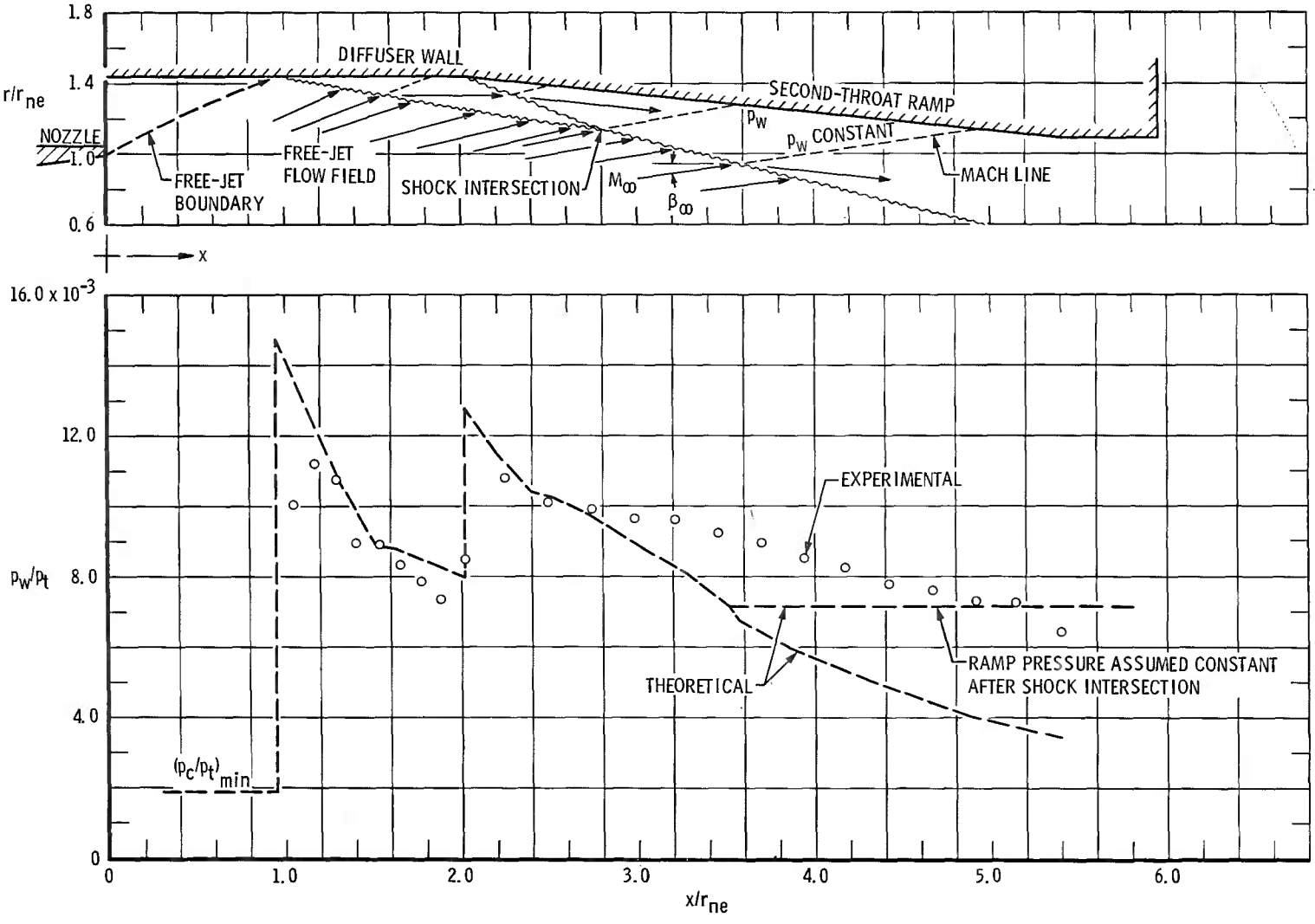

c. Configuration 3-6, $(L/D)_d = 0.70$

Fig. 11 Continued

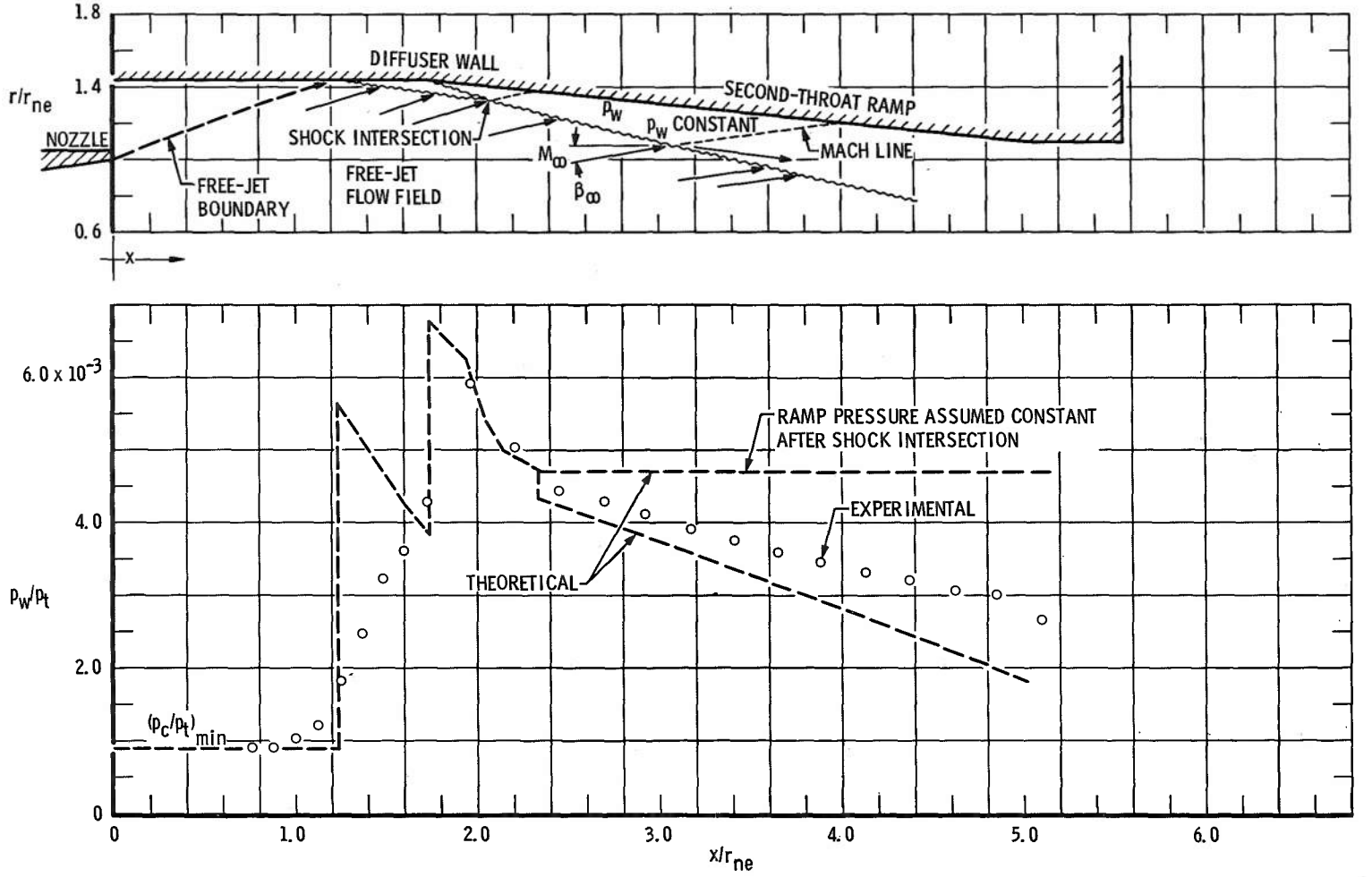

d. Configuration 4-6, $(L/D)_d = 0.60$

Fig. 11 Continued

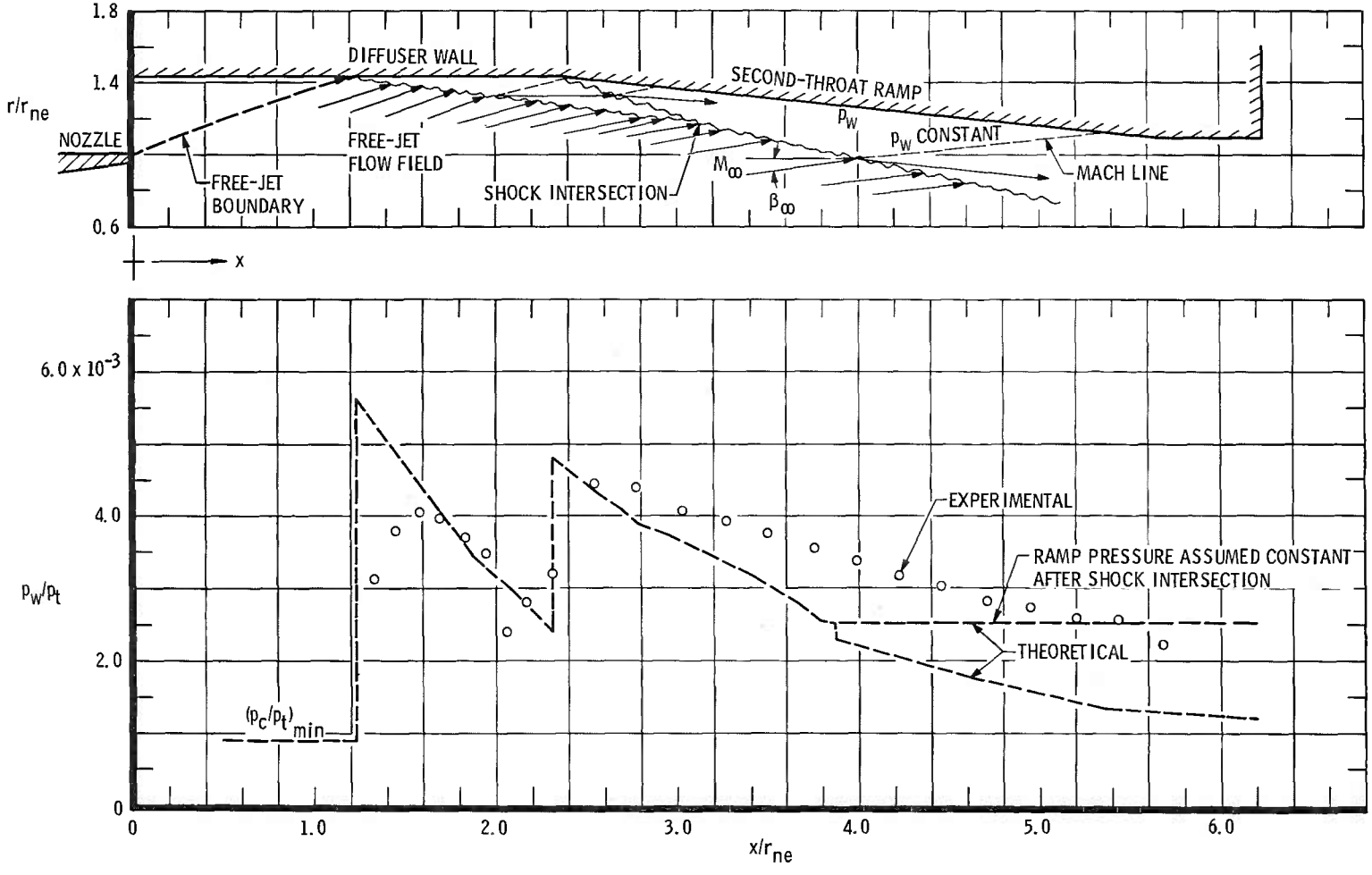

e. Configuration 4-6, $(L/D)_d = 0.80$

Fig. 11 Continued

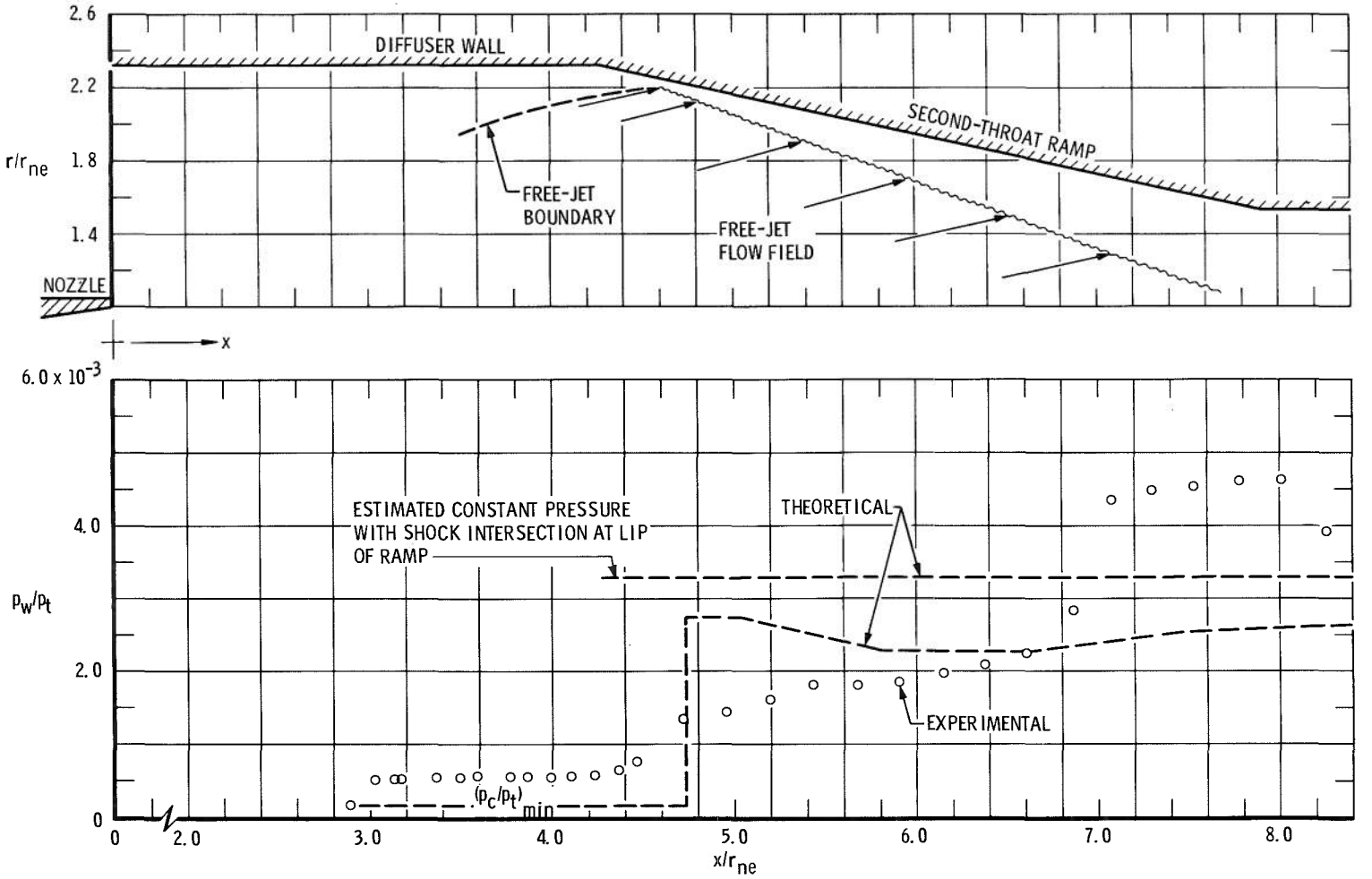

f. Configuration 5-5d, $(L/D)_d$ = 0.92

Fig. 11 Concluded

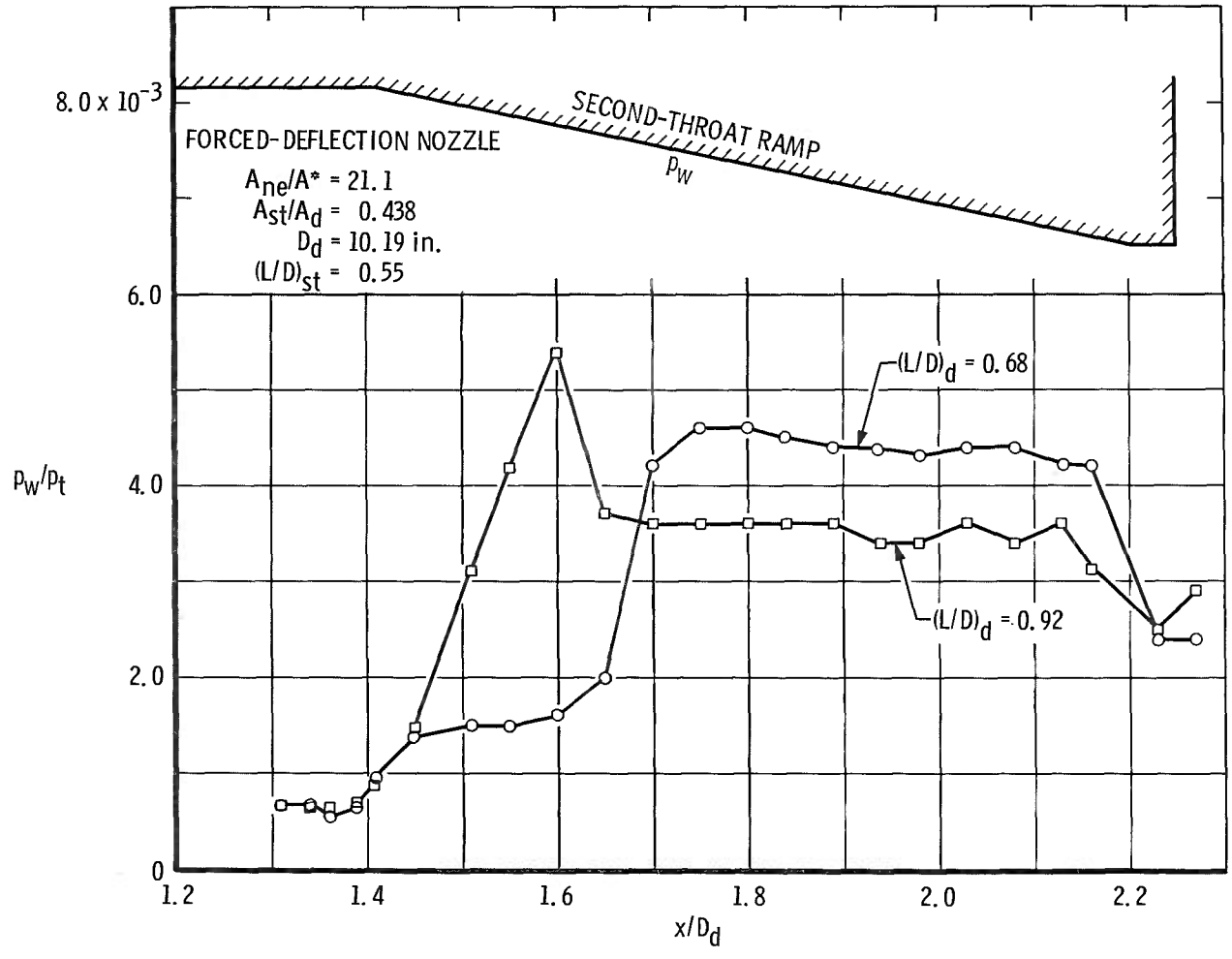

a. Configuration FD-5a

Fig. 12 Experimental Static Pressure Distributian an Second-Thraat Ramp for Annular and Cluster Nazzles at Various Second-Throat Positions (for Minimum P_{ex}/P_t)

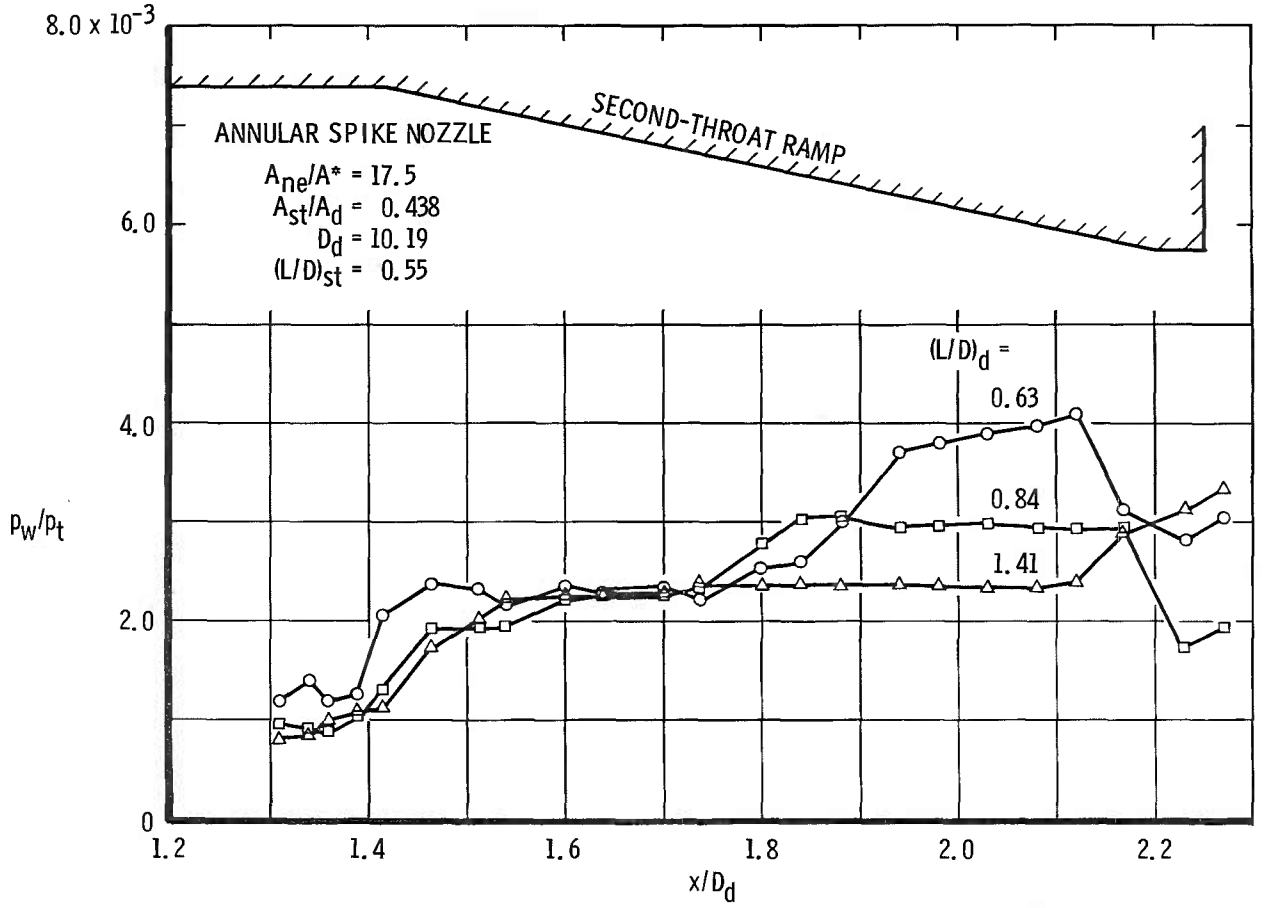

b. Configuration S2P1-5a

Fig. 12 Continued

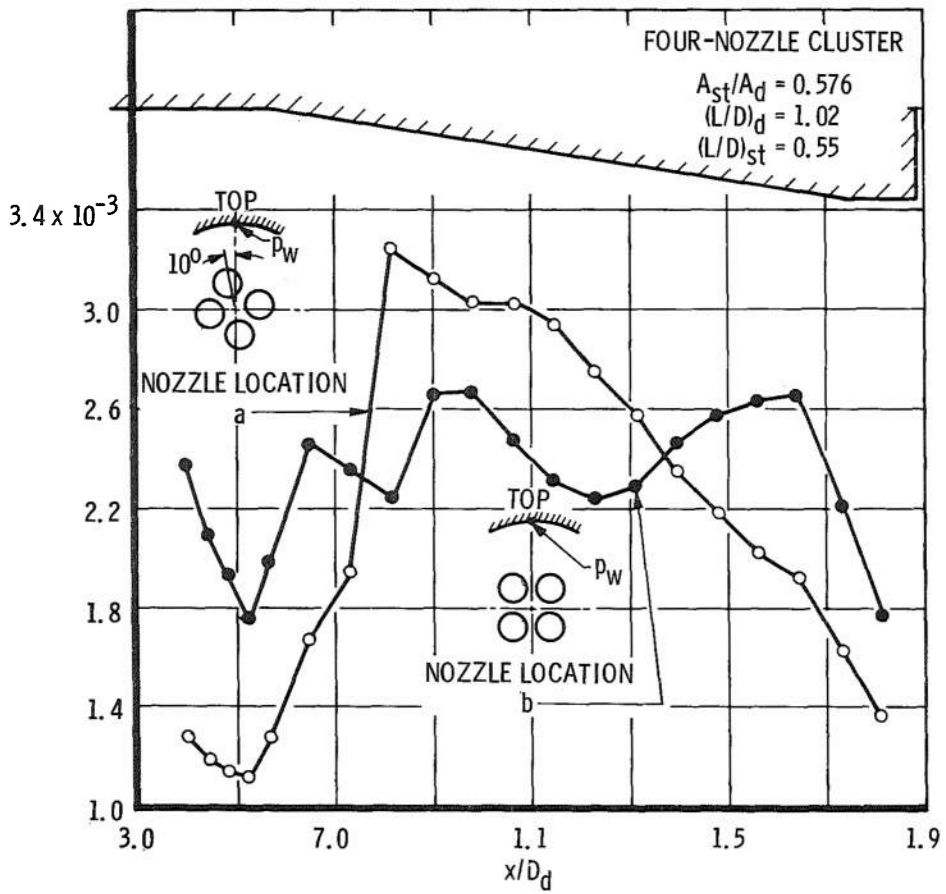

c. Configuration 9-6

Fig. 12 Concluded

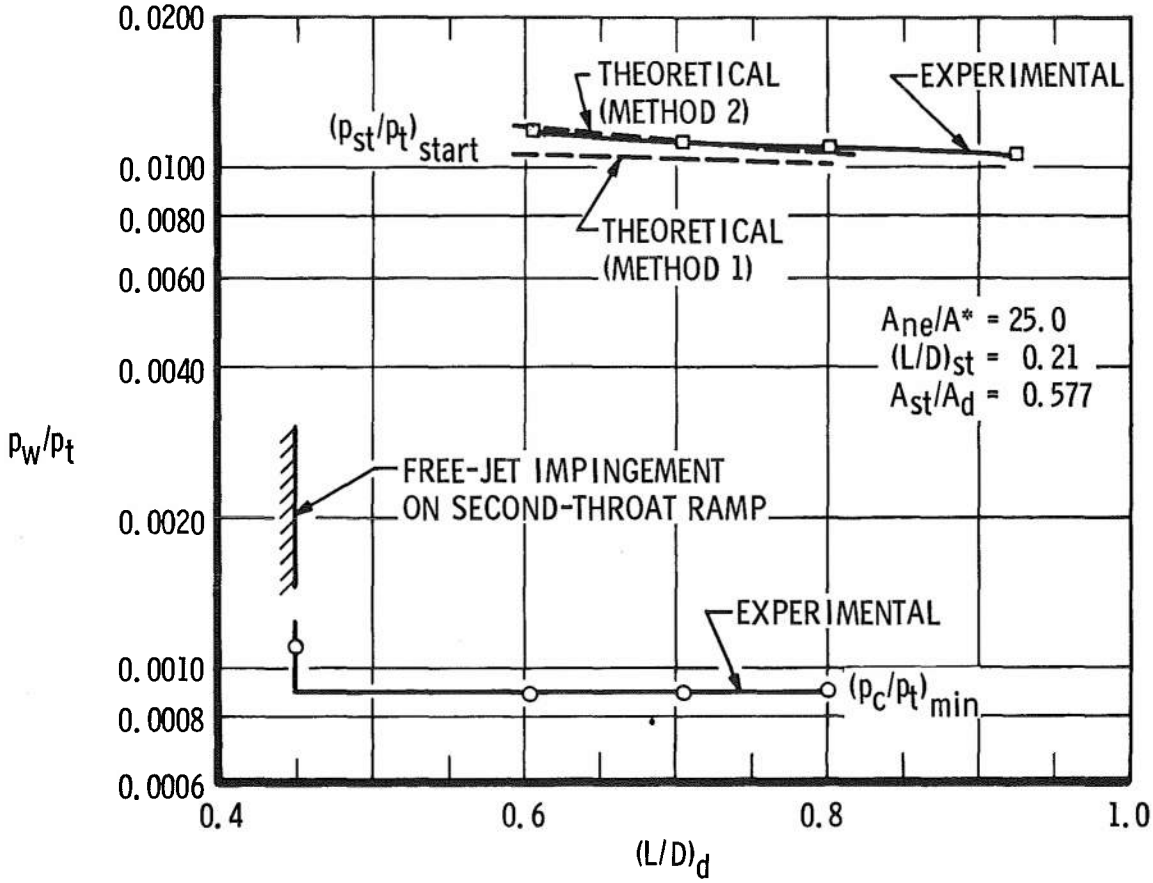

Fig. 13 Comparison of Experimental and Theoretical Second-Throat Starting Pressure Ratio (Configuration 4-6)

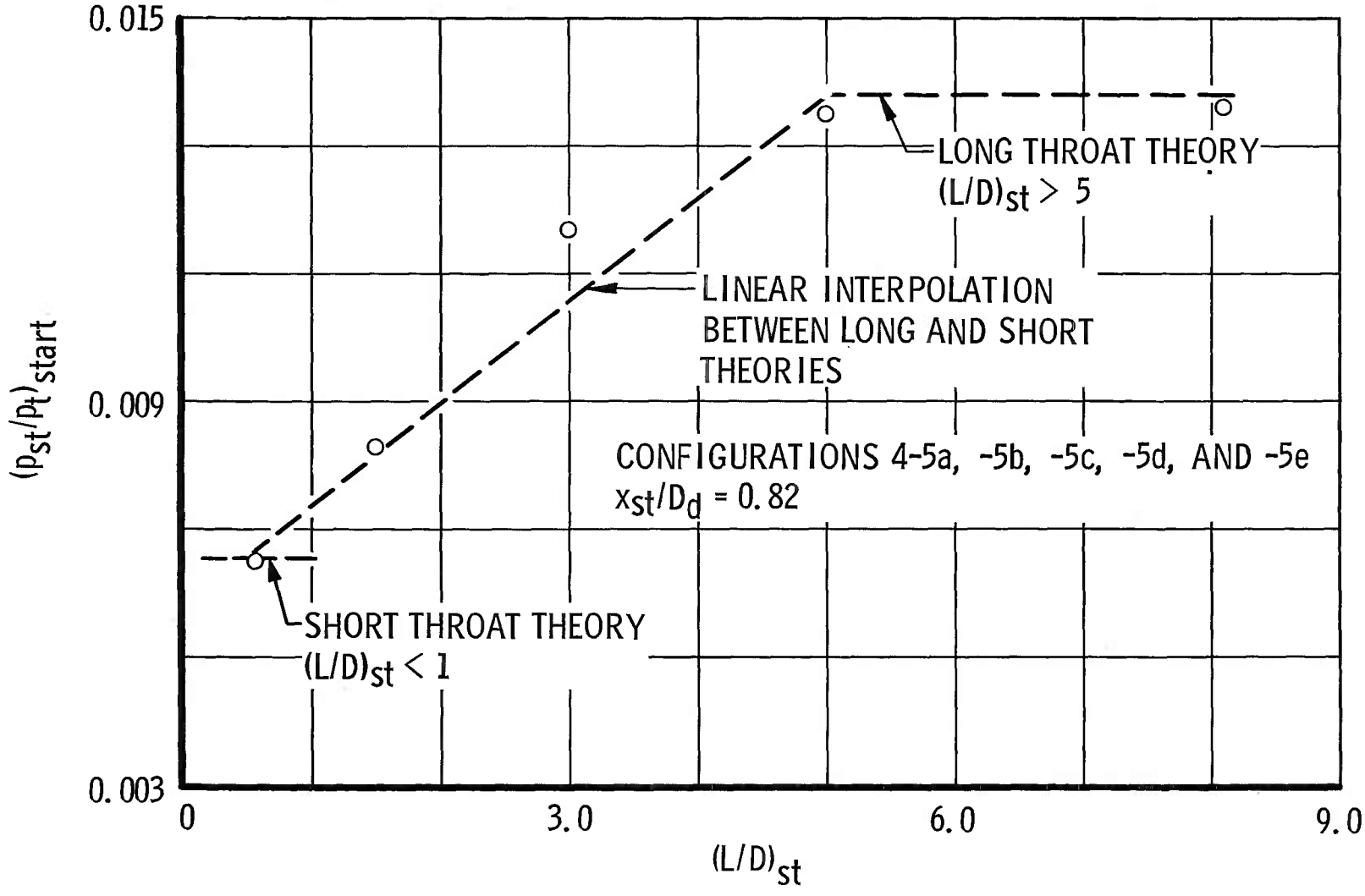

Fig. 14 Comparison of Experimental and Theoretical Intermediate Length Second-Throat Starting Pressure Ratio Using Linear Interpolation

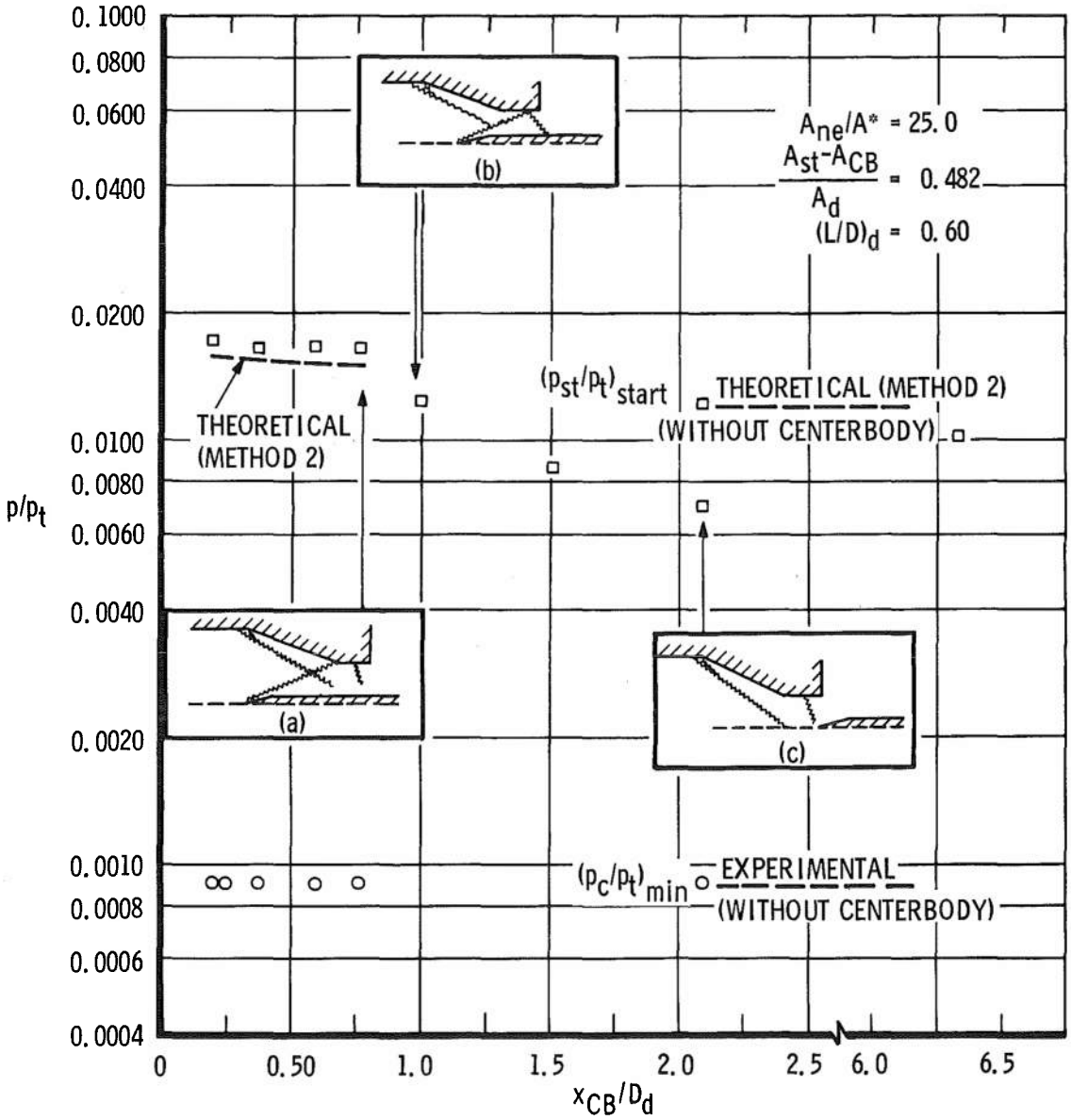

a. Configuration 4-6-CB

Fig. 15 Comparison of Experimental and Theoretical Second-Throat Starting Pressure Ratio with a Centerbody Located at Various Positions

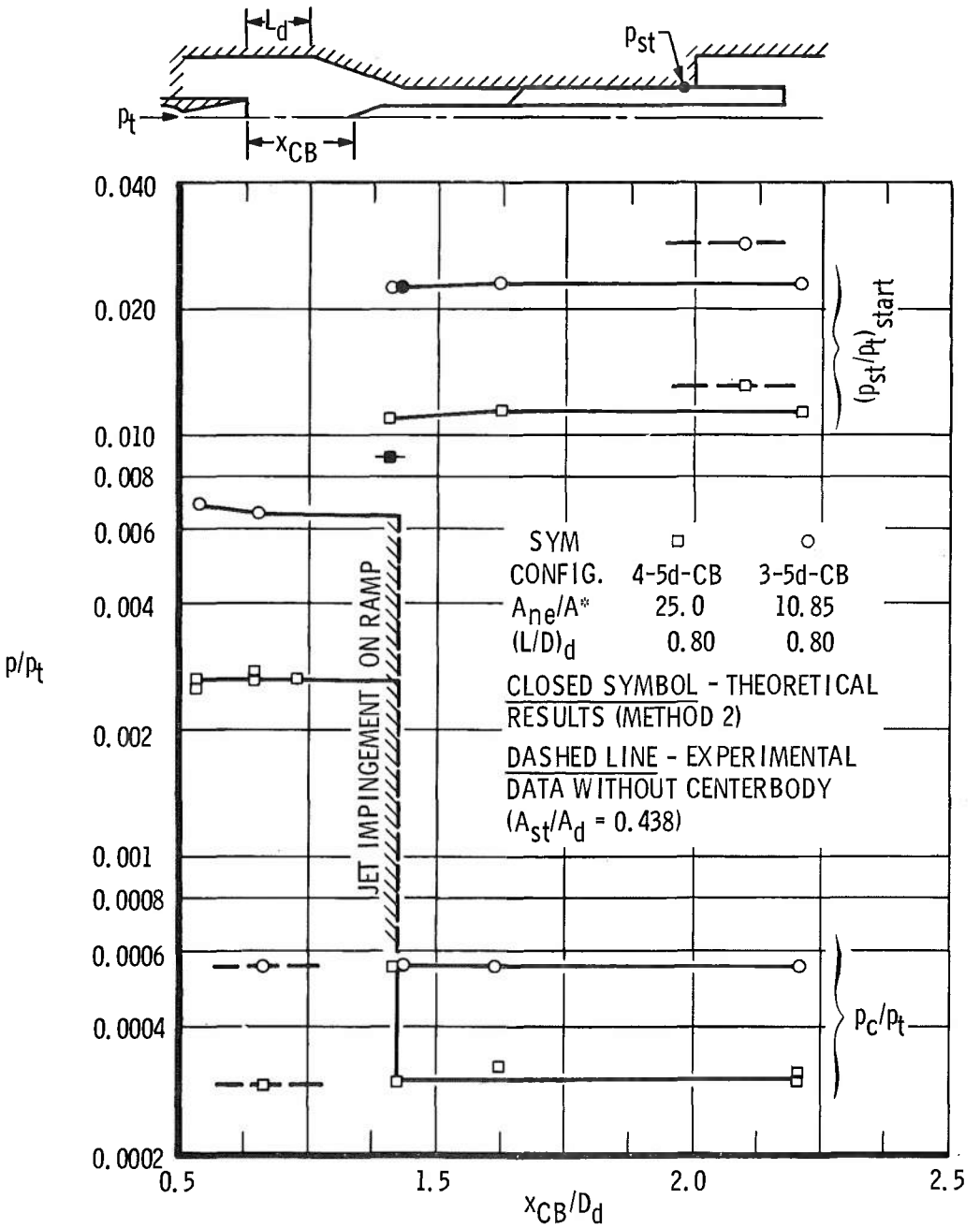

b. Configurations 3-5d-CB and 4-5d-CB

Fig. 15 Concluded

TABLE I
DESCRIPTION OF NOZZLES AND SECOND THROATS

a. Nozzle Dimensions

Config. Code	A_{ne}/A^*	A^*, in.^{2}	θ_{ne}, deg	D_{ne}, in.	Type Nozzle	Ref. Fig. No.
3+	10.85	1.251	18	4.16	Conical	7a
4+	25.00	0.542	18	4.16	Conical	7a
5+	23.68	0.636	0	4.38	Contour	7b
8+	18.57	0.754	18	4.21	Conical	7a
9+	10.7++	0.305	7.5++	1.00++	Four-Nozzle Cluster	7f
E-D	20.0	0.937	8	4.196	Annular	7c
F-D	21.1	0.654	8	4.196	Annular	7d
S2-P1	17.5	0.564	18.5	3.546	Annular	7e

b. Second-Throat Diffuser Dimensions

Config. Code	A_{st}/A_d	θ_R, deg	A_d, in.^{2}	$(L/D)_{st}$	$\frac{A_{st} - A_{CB}}{A_d}$	θ_{CB}	Ref. Fig. No.
5a	0.438	12	81.55	0.55	—	—	8a
5e	0.438	12	81.55	1.5	—	—	8a
5b	0.438	12	81.55	3.0	—	—	8a
5c	0.438	12	81.55	5.0	—	—	8a
5d	0.438	12	81.55	8.1	—	—	8a
5d-CB	0.438	12	81.55	8.1	0.417	18	8c
6	0.576	6	28.31	0.21	—	—	8a
6-CB	0.576	6	28.31	0.21	0.482	18	8b

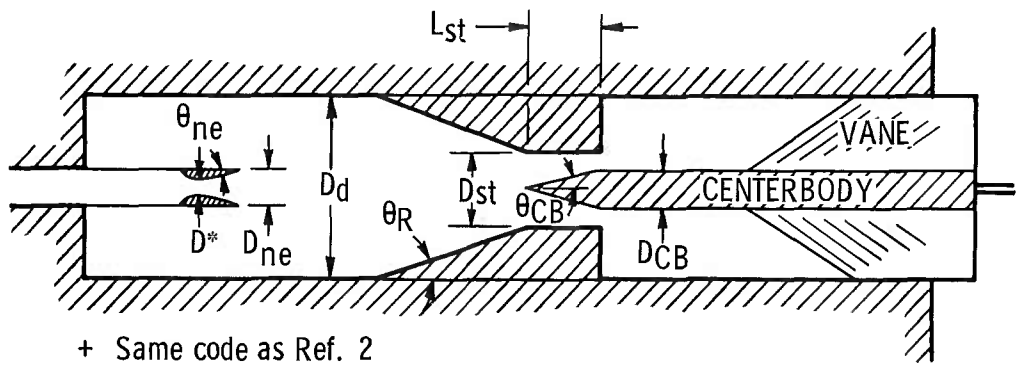

\+ Same code as Ref. 2

++ Description for each nozzle

TABLE II
COMPARISON OF EXPERIMENTAL AND THEORETICAL RESULTS
a. Long Second-Throat Performance

Config. Code	$\frac{A_{ne}}{A^*}$	D_d, in.	$\frac{A_{st}}{A_d}$	$(L/D)_{st}$	$\left(\frac{L}{D}\right)_d$	p_t, psia	Exper. (p_c/p_t)	Exper. (p_{st}/p_t) Start	Exper. (p_{st}/p_t) Oper.	Method 1		Method 2	
										Theory (p_{st}/p_t) Start	Percent Deviation	Theory (p_{st}/p_t) Start	Percent Deviation
3-5d	10.85	10.19	0.438	8.1	0.74	45.3	0.00056+	0.0280+	0.0280+	0.0252	- 9.7	0.0299	+6.8
3-5d	10.85				0.80	45.3	0.00056+	0.0285+	0.0285+	0.0288	+ 1.1	0.0297	+4.2
4-5d	25.0				0.80	44.9	0.00293+	0.0136+	0.0136+	0.0128	- 5.9	0.0138	+1.5
ED-5d	20.0				0.67	45.0	0.000223	0.0173	0.0173	0.0144	-16.8	—	—
					0.80		0.000224	0.0197	0.0197	0.0156	-20.8	—	—
					0.92		0.000224	0.0199	0.0199	0.0162	-18.6	—	—
ED-5d	20.0				1.17	45.0	0.000224	0.0189	0.0189	0.0175	-7.4	—	—
5-5d	23.68				0.80	44.8	0.000155	0.0169	0.0171	0.0181	+7.1	—	—
					0.86	45.0	0.000155	0.0167	0.0169	0.0181	+8.4	—	—
5-5d	23.68	10.19	0.438	8.1	0.92	45.0	0.000151	0.0162	0.0167	0.0181	+11.7	0.0166	+2.2
b. Short Second-Throat Performance													
3-5a	10.85	10.19	0.438	0.55	0.74	44.9	0.000551+	0.0169+	0.0175+	0.0165	-2.4	0.0166	-1.8
3-5a	10.85				0.80	44.9	0.000551+	0.0170+	0.0177+	0.0150	-13.3	0.0168	-1.2
4-5a	25.0				0.80	44.5	0.000299+	0.00648+	0.00665+	0.00636	-1.8	0.00656	+1.2
FD-5a	21.1				0.68	44.3	0.00016	0.0052	0.0068	—	—	—	—
FD-5a	21.1				0.92	44.4	0.00016	0.0053	0.0059	—	—	—	—
S2P1-5a	17.5				0.63	45.4	0.000280	0.00531	0.00543	0.00580	+9.0	—	—
					0.74	45.1	0.000276	0.00597	0.00598	0.00644	+7.9	—	—
S2P1-5a	17.5	10.19	0.438	0.55	1.41	45.4	0.000240	0.00356	0.00367	0.00541	+52.0	—	—
3-6	10.85	6.01	0.577	0.21	0.60	44.9	0.00204	0.0263	0.0298	0.0270	+2.6	—	—
3-6	10.85				0.70	44.8	0.00188	0.0275	0.0275	0.0268	-2.6	0.0283	+2.9
4-6	25.0				0.60	45.7	0.000888	0.0119	0.0119	0.01062	-12.0	0.0120	+0.8
4-6	25.0				0.80	45.5	0.000891	0.0107	0.0107	0.01025	-4.3	0.01092	+2.0
9-6	10.7	6.01	0.577	0.21	1.02	43.3	0.000392	0.00974	0.01095	0.00692	-29.0	—	—

+Data taken from Ref. 2

TABLE II (Continued)

c. Intermediate Length Second-Throat Performance (D_d = 10.19, A_{st}/A_d = 0.438)

Config. Code	$(L/D)_{st}$	$(L/D)_d$	p_t, psia	Exper. (p_c/p_t)	Exper. (p_{st}/p_t) Start	Exper. (p_{st}/p_t) Oper.	Exper. (p_{ex}/p_t) Start	Exper. (p_{ex}/p_t) Oper.	Method 1		Method 2	
									Theory (p_{ex}/p_t) Start	Percent Deviation	Theory (p_{ex}/p_t) Start	Percent Deviation
4-5e	1.50	1.18	44.12	—	0.00510	0.00596	0.00633	0.00664	0.00579	-9.3	—	—
↓	↓	1.06	44.12	—	0.00568	0.00580	0.00723	0.00735	0.00625	-13.5	—	—
↓	↓	0.94	44.12	—	0.00658	0.00718	0.00788	0.00815	0.00713	-9.5	—	—
4-5e	1.50	0.82	44.02	—	0.00830	0.00850	0.00857	0.00892	0.00826	-3.6	0.00950	+10.40
4-5b	3.00	1.18	44.07	0.000280	0.00663	0.00714	0.00878	0.00900	0.00975	+11.0	—	—
↓	↓	0.94	44.33	0.000274	0.01167	0.01177	0.01090	0.01130	0.01070	-1.8	—	—
4-5b	3.00	0.82	44.23	—	0.00933	0.00991	0.01240	0.01250	0.01146	-7.3	0.0129	+4.00
4-5c	5.00	1.06	44.23	0.000276	0.01322	0.0134	0.01350	0.01360	0.01411	+4.5	—	—
↓	↓	0.94	44.12	0.000268	—	—	0.01370	0.01370	0.01397	+2.0	—	—
4-5c	5.00	0.82	44.43	0.000267	—	—	0.01350	0.01350	0.01381	+2.2	0.01372	+1.60
F-D-5b	3.00	1.18	42.93	0.000207	—	—	0.01380	0.01400	—	—	—	—
↓	↓	0.94	42.93	0.000207	—	—	0.01390	0.01510	—	—	—	—
↓	↓	0.82	42.93	0.000198	—	—	0.01320	0.01650	—	—	—	—
↓	↓	0.79	42.93	0.000166	—	—	0.01320	0.01590	—	—	—	—
F-D-5b	3.00	0.70	42.93	0.000133	—	—	0.01300	0.01660	—	—	—	—
S2-P1-5b	3.00	0.36	44.32	0.000292	—	—	0.01000	0.01040	—	—	—	—
S2-P1-5b	3.00	0.23	44.42	0.000294	—	—	0.01090	0.01110	—	—	—	—
8-5b	3.00	1.42	45.52	0.000360	—	—	0.01280	0.01350	—	—	—	—
↓	↓	1.18	45.42	0.000345	—	—	0.01430	0.01440	—	—	—	—
↓	↓	0.94	45.42	—	—	—	0.01460	0.01500	—	—	—	—
↓	↓	0.82	45.42	0.000361	—	—	0.01650	0.01670	0.01575	-4.5	—	—
8-5b	3.00	0.70	45.37	0.000353	—	—	0.01580	0.01600	0.01572	-0.5	—	—

TABLE II (Concluded)

d. Centerbody Performance

Config. Code	A/A*	Dd, in.	A_{st}/A_d	$(L/D)_{st}$	$\left(\frac{L}{D}\right)_d$	$\frac{A_{st} - A_{CB}}{A_d}$	$\frac{X_{CB}}{D_d}$	pt, psia	Exper. (p_c/p_t)	Exper. (p_{st}/p_t) Start	Exper. (p_{st}/p_t) Oper.	Method 2 Theory (p_{st}/p_t) Start	Method 2 Percent Deviation
3-5d-CB	10.85	10.19	0.438	8.10	0.80	0.417	1.35	45.2	—	LIMIT Ejec. will not restart		LIMIT Ejec. will not restart	
↓	↓	↓	↓	↓	↓	↓	1.37	45.2	0.00055	0.0228	0.0228	0.02280	0
4-5d-CB	25.00	10.19	0.438	8.10	0.80	0.417	1.33	44.6	—	LIMIT		LIMIT	
↓	↓	↓	↓	↓	↓	↓	1.35	44.8	0.00030	0.0110	0.0110	0.00895	-10.5
3-6-CB	10.85	6.01	0.577	0.21	0.70	0.482	0.40	44.8	0.00190	0.0375	0.0382	0.0363	-3.20
↓	↓	↓	↓	↓	↓	↓	0.68	45.4	0.00189	0.0390	0.0404	0.0357	-8.50
↓	↓	↓	↓	↓	↓	↓	1.00	45.0	0.00184	0.0272	0.0274	0.0283	+4.00
4-6-CB	25.00	6.01	0.577	0.21	0.60	0.482	0.20	45.7	0.00090	0.0172	0.0175	0.01575	-7.40
↓	↓	↓	↓	↓	↓	↓	0.77	45.2	0.00090	0.0165	0.0166	0.01470	-10.90
↓	↓	↓	↓	↓	↓	↓	1.00	45.6	0.00090	0.0124	0.0125	0.01200	-2.40

TABLE III
DESCRIPTION OF MEASURING INSTRUMENTS

Parameter Measured	Range Measured	Measuring Instrument
p_c	0.2 to 5 mm HgA	McLeod (with Nitrogen Cold Trap)
	5 to 50 mm HgA	Diaphragm-Activated Dial Gage
p_{ex}, p_{st}, and p_s	7 to 50 mm HgA	Diaphragm-Activated Dial Gage
	1 to 10 psia	Diaphragm-Activated Dial Gage
p_t	1 to 46 psia	Diaphragm-Activated Dial Gage
p_w, p_R, and p_{t_r}	0.1 to 90 in. (Oil)	Manometer (Silicone Oil-sp gr = 1.092 at 80°F)
T_t	70 to 100°F	Copper-Constantan Thermocouple
p_{t_r}	0.2 to 33 in. HgA	Manometer (Mercury)

APPENDIX I
INTERMEDIATE LENGTH SECOND-THROAT MATHEMATICAL FLOW MODEL DEVELOPMENT

Because of the complexity of the intermediate length diffuser flow field, a mathematical flow model was developed to aid in calculating the starting pressure ratio for intermediate length second-throat diffusers. This model is essentially an interpolation of the two flow models assumed for short and long second throats. The following sketch shows typical flow models which could be assumed for long and short second-throat diffusers.

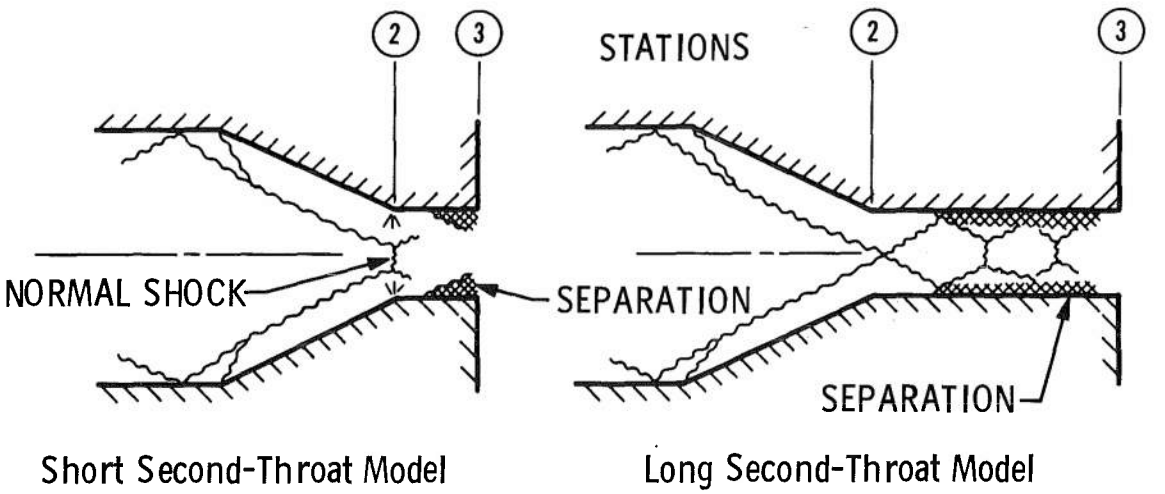

The long second-throat model assumes the flow shocks down, with one-dimensional subsonic flow existing at station 3. The short second-throat model assumes a normal shock at station 2. Both flow models assume separation of the turbulent boundary layer along the diffuser walls. These two flow models were substantiated only partially experimentally and are, therefore, offered as one possible description of the phenomena that actually take place.

INTERMEDIATE LENGTH SECOND-THROAT RAKE STUDY

The total pressure profile was obtained at the exit of the second-throat diffuser in an attempt to learn more about the flow structure at station 3 for various throat lengths, as shown in the sketch on the following page.

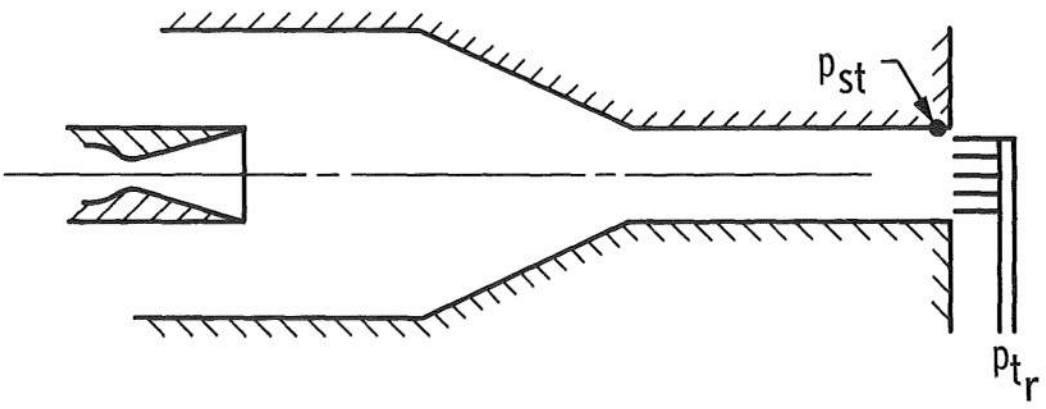

Typical Second-Throat Rake Installation

Figure I-1 shows the total pressure profiles which were taken at the exit of second-throat configurations 4-5a, -5b, -5c, and -5e, at various nozzle positions.

There are two methods for calculating the stream Mach number. One method uses the measured static and rake total pressures, and the other uses the measured rake and nozzle total pressures. Whether subsonic or supersonic flow exists can definitely be determined by the first method. However, it is impossible to determine from total pressure measurements alone if the measured total pressure loss was due to a normal standing in the second throat (subsonic solution) or to a probe-induced shock (supersonic solution). An examination of the measured total pressure profiles shown in Fig. I-1a shows relative uniform profiles for second-throat lengths of $(L/D)_{st}$ = 5 and 3. It should be noted that the pressure profiles shown in Figs. I-1a and b were made just prior to unstarting the ejector system. An assumption was, therefore, made that the measured wall static pressure for these configurations was equal to the stream static pressure at this station. The calculated pressure ratio, p_{st}/p_{t_r}, indicated that the flow was definitely subsonic. However, when rake measurements were made for second-throat lengths of $(L/D)_{st}$ = 1.5 and 0.55, a definite change in the profile was noted, and the stream static pressure could not be assumed equal to the wall static pressure. Although it cannot be determined definitely that supersonic or subsonic flow exists at station 3 from the rake data, it is feasible that a subsonic core could exist for the short throat configuration.

FLOW MODEL EQUATIONS

A mathematical flow model was developed based on the experimental observations and the premise that the subsonic flow could exist

at station 3 for both long and short second-throat diffusers.

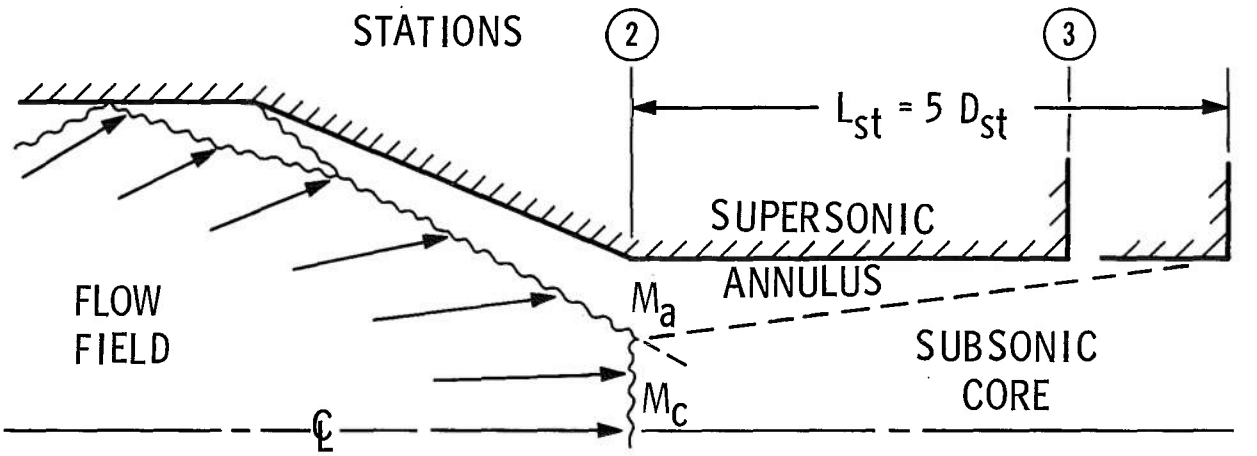

This model assumes a uniform subsonic core surrounded by a uniform supersonic annulus with both regions at the same static pressure. It should be noted that the various intermediate second-throat lengths probably do not have a pure subsonic core just prior to starting; however, the model merely assumes the subsonic Mach number which would exist at station 3 if the flow were to shock down between stations 2 and 3 for each intermediate length.

By making additional assumptions of

1. Steady flow,
2. Perfect gas, and
3. Adiabatic flow,

the conservation equations may be written as

$$\frac{F_{3_x}}{\dot{m}\sqrt{R\,T_t}} = \frac{A_c\,(1+\gamma\,M_c^2) + (A_{st}-A_c)\,(1+\gamma\,M_a^2)}{A_c\,M_c\sqrt{\gamma\left(1+\frac{\gamma-1}{2}\,M_c^2\right)} + (A_{st}-A_c)\,M_a\sqrt{\gamma\left(1+\frac{\gamma-1}{2}\,M_a^2\right)}} \qquad \text{(I-1)}$$

In addition, it is assumed that the subsonic core is formed by a normal shock at station 2, the size of which is determined by the position of the ramp shock at this station. Both the position of the ramp shock at station 2 and $F3_x$ can be obtained from the previous theoretical calculations of the forces upstream of the throat entrance using Method 2. The subsonic core Mach number, M_c, at station 2 can be found by the normal shock relations for the existing supersonic free-stream centerline Mach number, $M_{℄}$, at station 2. This allows the solution of the supersonic Mach number in the annulus, M_a, at station 2. If the flow field approaching the second throat is not available, the following section provides an alternate semi-empirical solution which works reasonably well for nozzles with uniform exit conditions.

In order to solve Eq. (I-1) at station 3, two additional assumptions are made.

1. A linear decrease of M_a from the calculated value at station 2 to a value of unity of five diameters downstream and
2. A linear growth of A_c from the calculated value at station 2 to A_{st} at five diameters downstream.

The maximum starting diffuser exit pressure ratio for any given second-throat length between $(L/D)_{st} = 1$ and 5 may now be calculated from

$$\frac{p_{st}}{p_t} = \frac{\dot{m}\sqrt{RT_t}/p_t}{A_{c_3} M_{c_3}\sqrt{\gamma\left(1 + \frac{\gamma-1}{2} M_{c_3}^2\right)} + (A_{st} - A_{c_3}) M_{a_3}\sqrt{\gamma\left(1 + \frac{\gamma-1}{2} M_{a_3}^2\right)}} \tag{I-2}$$

SEMI-EMPIRICAL METHOD FOR DETERMINING CONDITIONS AT THROAT ENTRANCE

Both the size of the normal shock disk assumed at station 2 and the Mach number approaching this disk must be determined in order to solve the intermediate length second-throat starting model. The core Mach number approaching this disk may be rigorously determined by a straight forward application of an irrotational inviscid characteristics solution. If a conical nozzle is used as the driving nozzle, the centerline Mach number distribution may rigorously be determined from a simple closed form solution. This method is based on the fact that the free-jet core flow is conical in nature until the first expansion line from the nozzle lip crosses the nozzle centerline. For a high area ratio nozzle, this point is generally downstream of station 2. The fact that the centerline flow is conical resolves to the following equation:

$$\frac{A_x}{A^*} = \frac{A_{ne}}{A^*}\left[1 - 2\sin^2\left(\frac{\theta_{ne}}{2}\right) + \frac{X}{r_{ne}}\sin\theta_{ne}\right]^2 \tag{I-3}$$

where A_X/A^* is the expansion area ratio experienced by the gas on the nozzle centerline and X is the distance downstream of the nozzle exit. The centerline Mach number distribution may then be determined using isentropic compressible flow tables.

Location of the ramp shock at station 2 is considerably more difficult because the nonuniform flow field from the nozzle at this station causes the flow to be rotational behind the shock. A semi-empirical solution of the shock location at station 2 assumes the ramp shock is two-dimensional(straight) and emanates half-way between the jet

impingement point and the ramp leading edge. It is further assumed that the gas expands from the nozzle to a mean gas expansion angle (θ_m) and is turned parallel to the second-throat ramp through the two-dimensional oblique shock system. This mean gas expansion angle (θ_m) was developed in Ref. 2 for estimating ramp pressure area drag and may be calculated from the following equation:

$$\theta_m = \tan^{-1}\left[\frac{\sqrt{\frac{A_{st}}{A_d}+1}}{2\sqrt{2}\left(\frac{X_n}{D_d}+\frac{X_{st}}{D_d}\right)+\frac{\sqrt{2}-\sqrt{\frac{A_{st}}{A_d}+1}}{\tan\theta_{st}}}\right] \quad \text{(I-4)}$$

The Mach number used with the mean gas expansion angle is the isentropic value based on the area ratio, A_d/A^*.

COMPARISON OF EXPERIMENTAL AND THEORETICAL INTERMEDIATE LENGTH SECOND-THROAT PERFORMANCE

The majority of the investigation of a theoretical method for calculating intermediate length second-throat performance was accomplished using Method 1, as is evident from the comparisons of theoretical and experimental starting pressure ratios in Figs. I-2a and b and as tabulated in Table II. Figure I-2a compares the results using Method 1 and the intermediate length second-throat flow model with the available conical nozzle starting pressure ratio data for optimum second-throat positions. If the gross simplification of the flow model is considered, good agreement was obtained between the experimental and theoretical results.

It is anticipated that Method 2 will be required for nozzles whose exit Mach number distributions are nonuniform. Figure I-2a shows a comparison of both methods for the $A_{ne}/A^* = 25.0$ conical nozzle. Both Method 1 and 2 agreed with the experimental results within approximately 10 percent. Table II shows that the percentage varies with the second-throat length.

Figure I-2b compares the theoretical and experimental second-throat starting pressure ratios at various second-throat positions for the $A_{ne}/A^* = 25.0$ conical nozzle using Method 1. The maximum error (12-percent deviation) was found at the maximum X_{st}/D_d. The maximum error at this point is thought to be the result of the assumptions that the normal shock disk is located at station 2 and in the method used to calculate the size of this disk. The assumption of uniform static pressure at each station, also, is less valid at minimum $(L/D)_{st}$. Because of these discrepancies in the assumptions at small values of $(L/D)_{st}$, it is recommended that the short second-throat theory described in section 2.2.1 be used for $(L/D)_{st}$ less than one.

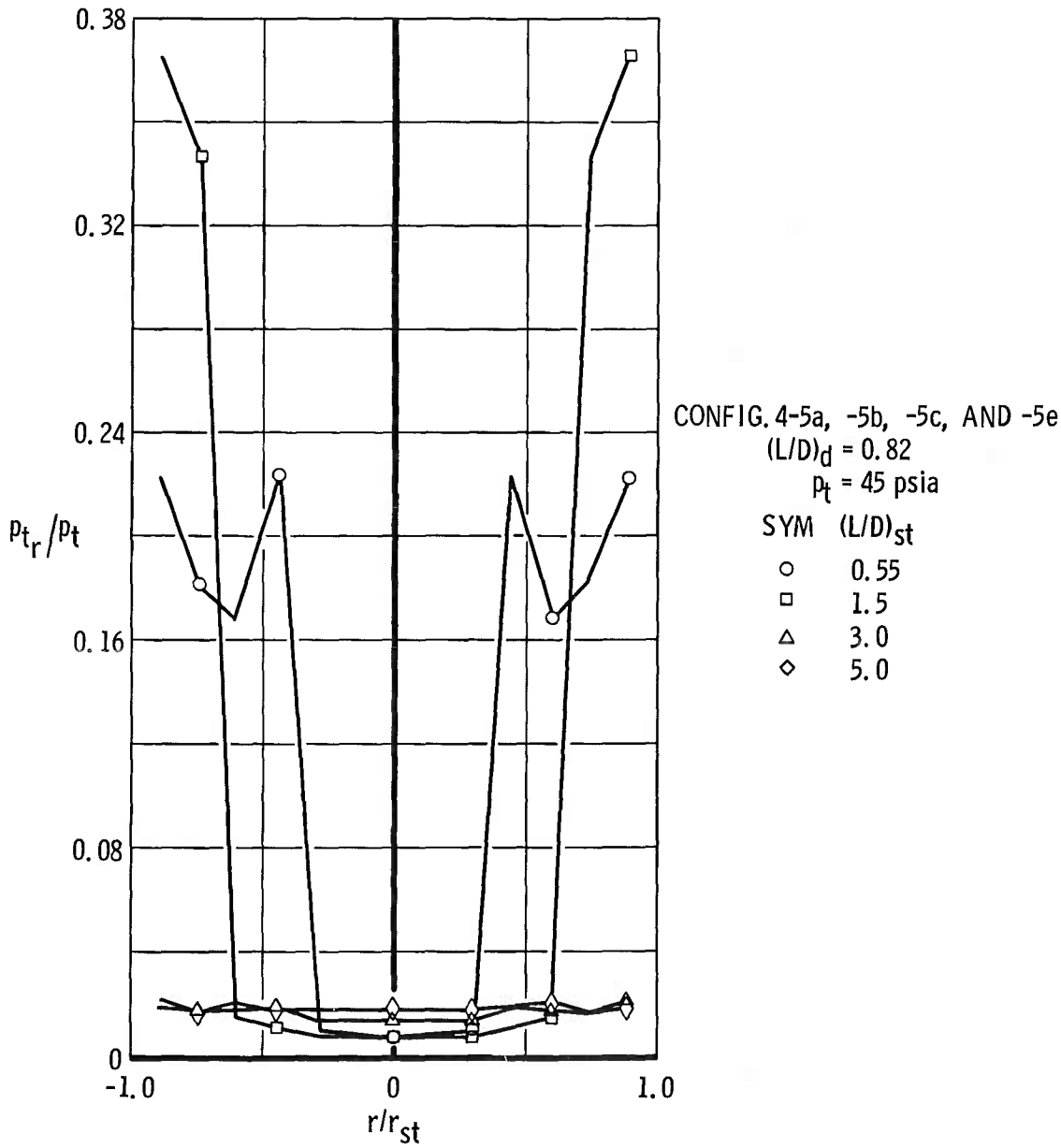

a. Effect of Throat Length

Fig. I-1 Experimental Total Pressure Profiles at Second-Throat Exit

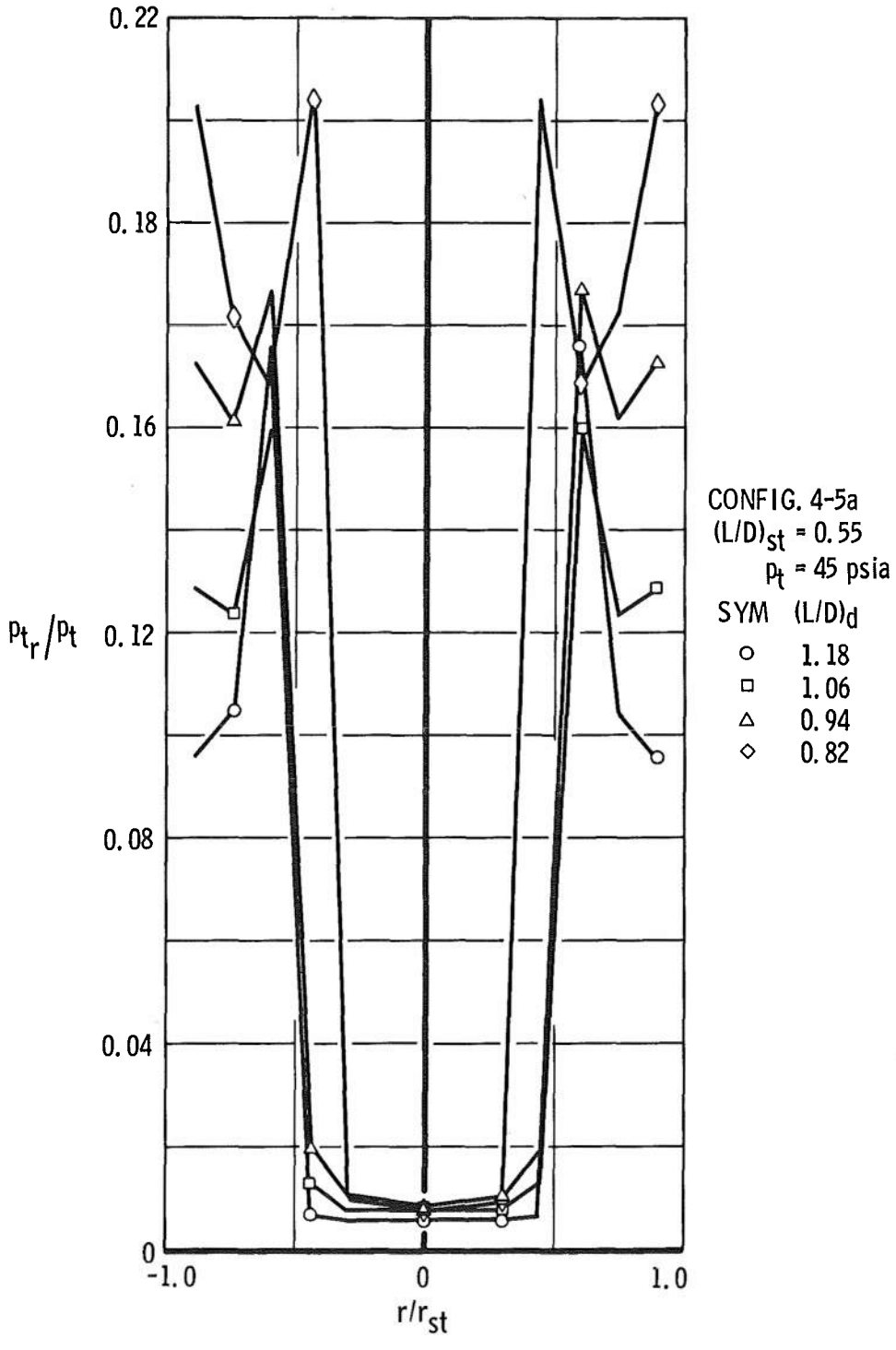

b. Effect of Second-Throat Position

Fig. I-1 Concluded

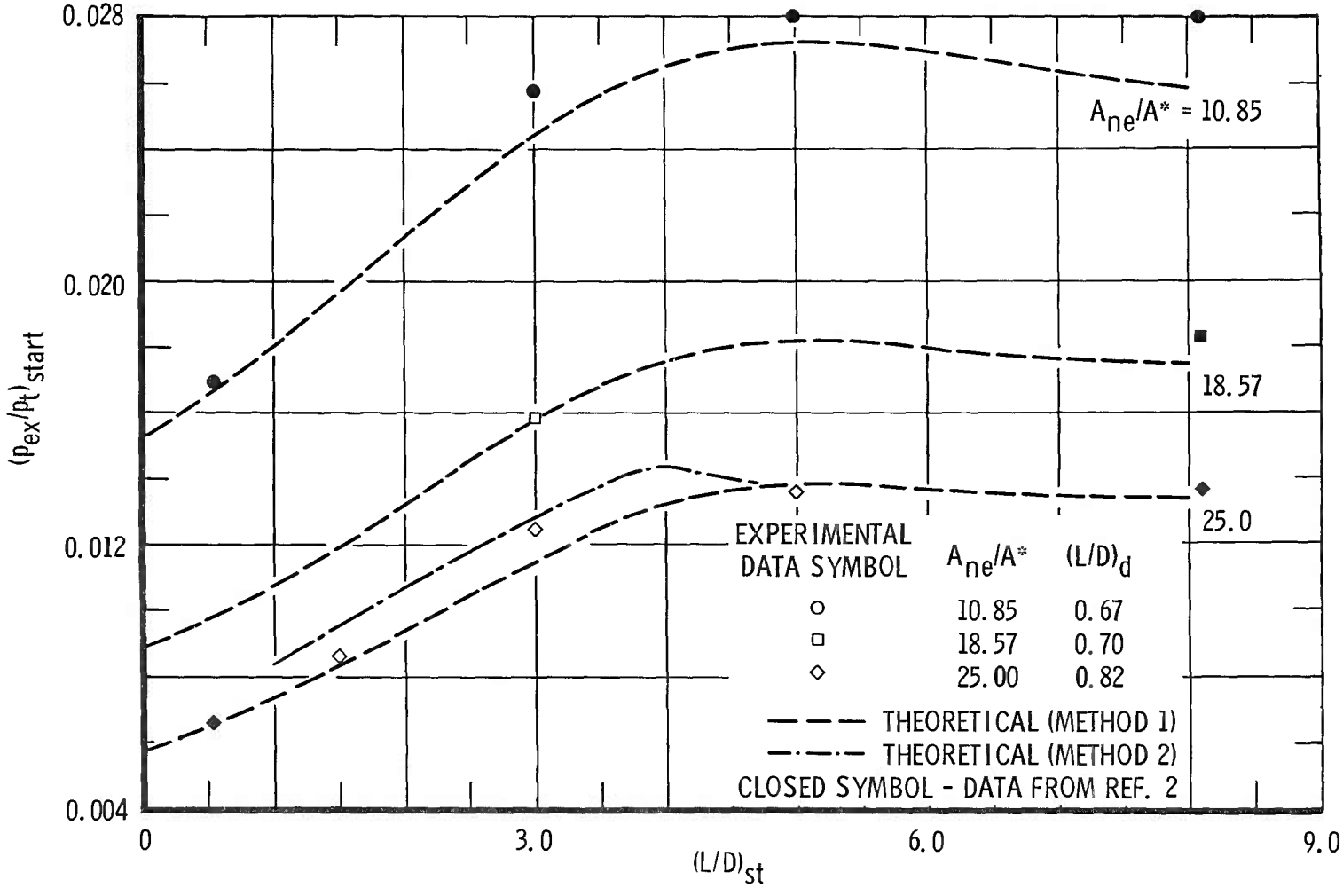

a. Nozzle Configurations 3, 4, and 8

Fig. I-2 Comparison of Theoretical and Experimental Starting Pressure Ratio for Intermediate Length Second-Throat Diffusers

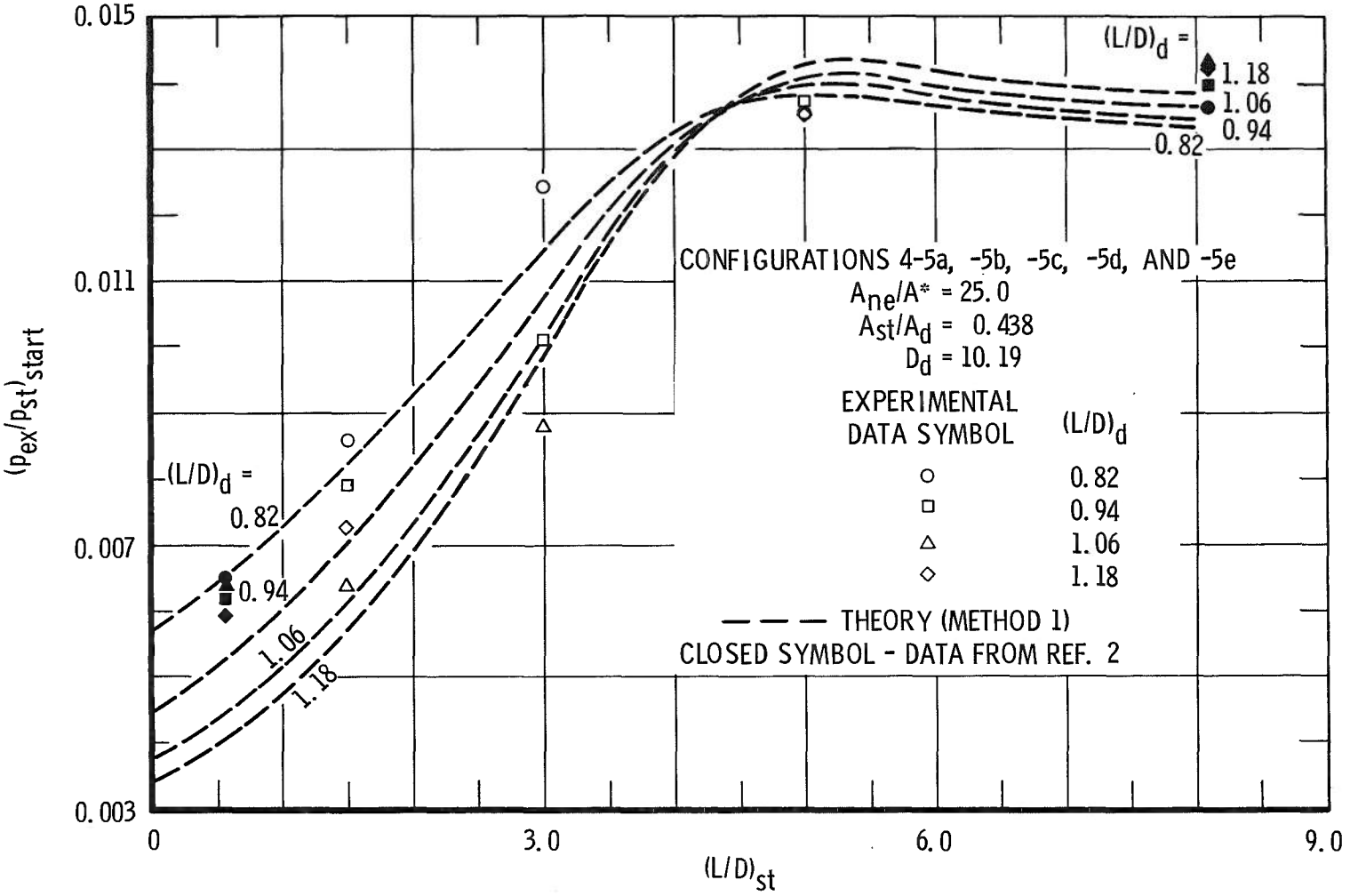

b. Effect of Second-Throat Position

Fig. I-2 Concluded

UNCLASSIFIED

Security Classification

DOCUMENT CONTROL DATA - R&D

(Security classification of title, body of abstract and indexing annotation must be entered when the overall report is classified)

1. ORIGINATING ACTIVITY (Corporate author)	2a. REPORT SECURITY CLASSIFICATION
Arnold Engineering Development Center, ARO, Inc., Operating Contractor, Arnold Air Force Station, Tennessee	UNCLASSIFIED
	2b. GROUP N/A

3. REPORT TITLE

IMPROVED METHODS FOR DETERMINING SECOND-THROAT DIFFUSER PERFORMANCE OF ZERO-SECONDARY-FLOW EJECTOR SYSTEMS

4. DESCRIPTIVE NOTES (Type of report and inclusive dates)

N/A

5. AUTHOR(S) (Last name, first name, initial)

German, R. C., and Panesci, J. H., ARO, Inc.

6. REPORT DATE	7a. TOTAL NO. OF PAGES	7b. NO. OF REFS
July 1965	64	7

8a. CONTRACT OR GRANT NO.	9a. ORIGINATOR'S REPORT NUMBER(S)
AF 40(600)-1000	
b. PROJECT NO. 6950	AEDC-TR-65-124
c. Program Element 62405184	9b. OTHER REPORT NO(S) (Any other numbers that may be assigned this report)
d. Task 695002	N/A

10. AVAILABILITY/LIMITATION NOTICES

Qualified requesters may obtain copies of this report from DDC. DDC release to CFSTI and foreign announcement and distribution of this report are not authorized.

11. SUPPLEMENTARY NOTES	12. SPONSORING MILITARY ACTIVITY
N/A	Arnold Engineering Development Center, Air Force Systems Command, Arnold Air Force Station, Tennessee

13. ABSTRACT

Improved methods are presented for estimating the required starting pressure ratio of a given axisymmetric second-throat, ejector-diffuser system used in rocket altitude simulation. The improved theory involves a more accurate technique for determining ramp pressure. The new technique utilizes the flow field approaching the second throat along with two-dimensional oblique shock relations and the conservation equations to determine the conditions at the throat entrance. The results are applied to second-throat diffusers with throat lengths varying from 0.2 to 8.1 throat diameters and to second throats with a center-body located at various positions. A comparison of the theoretical starting pressure ratios with the experimental data from previous work, as well as the additional experimental data obtained during this investigation, gave a maximum deviation of less than 10 percent for most of the configurations investigated. The improved method should be especially applicable to ejector-diffuser systems whose nozzle exit flow fields are nonuniform, such as exist in annular and clustered driving nozzles.

This document has been approved for public release and its distribution is unlimited. Per A. F. Letter dtd 13 May 74 Signed William O. Cole

DD FORM 1 JAN 64 1473

UNCLASSIFIED

Security Classification

14. KEY WORDS	LINK A		LINK B		LINK C	
	ROLE	WT	ROLE	WT	ROLE	WT
diffusers						
second throat						
starting pressure ratios						
ejector systems						
zero secondary flow						
performance						
altitude simulation						

INSTRUCTIONS

1. ORIGINATING ACTIVITY: Enter the name and address of the contractor, subcontractor, grantee, Department of Defense activity or other organization *(corporate author)* issuing the report.

2*a*. REPORT SECURITY CLASSIFICATION: Enter the overall security classification of the report. Indicate whether "Restricted Data" is included. Marking is to be in accordance with appropriate security regulations.

2*b*. GROUP: Automatic downgrading is specified in DoD Directive 5200.10 and Armed Forces Industrial Manual. Enter the group number. Also, when applicable, show that optional markings have been used for Group 3 and Group 4 as authorized.

3. REPORT TITLE: Enter the complete report title in all capital letters. Titles in all cases should be unclassified. If a meaningful title cannot be selected without classification, show title classification in all capitals in parenthesis immediately following the title.

4. DESCRIPTIVE NOTES: If appropriate, enter the type of report, e.g., interim, progress, summary, annual, or final. Give the inclusive dates when a specific reporting period is covered.

5. AUTHOR(S): Enter the name(s) of author(s) as shown on or in the report. Enter last name, first name, middle initial. If military, show rank and branch of service. The name of the principal author is an absolute minimum requirement.

6. REPORT DATE: Enter the date of the report as day, month, year, or month, year. If more than one date appears on the report, use date of publication.

7*a*. TOTAL NUMBER OF PAGES: The total page count should follow normal pagination procedures, i.e., enter the number of pages containing information.

7*b*. NUMBER OF REFERENCES: Enter the total number of references cited in the report.

8*a*. CONTRACT OR GRANT NUMBER: If appropriate, enter the applicable number of the contract or grant under which the report was written.

8*b*, 8*c*, & 8*d*. PROJECT NUMBER: Enter the appropriate military department identification, such as project number, subproject number, system numbers, task number, etc.

9*a*. ORIGINATOR'S REPORT NUMBER(S): Enter the official report number by which the document will be identified and controlled by the originating activity. This number must be unique to this report.

9*b*. OTHER REPORT NUMBER(S): If the report has been assigned any other report numbers *(either by the originator or by the sponsor)*, also enter this number(s).

10. AVAILABILITY/LIMITATION NOTICES: Enter any limitations on further dissemination of the report, other than those imposed by security classification, using **standard** statements such as:

(1) "Qualified requesters may obtain copies of this report from DDC."

(2) "Foreign announcement and dissemination of this report by DDC is not authorized."

(3) "U. S. Government agencies may obtain copies of this report directly from DDC. Other qualified DDC users shall request through _____."

(4) "U. S. military agencies may obtain copies of this report directly from DDC. Other qualified users shall request through _____."

(5) "All distribution of this report is controlled. Qualified DDC users shall request through _____."

If the report has been furnished to the Office of Technical Services, Department of Commerce, for sale to the public, indicate this fact and enter the price, if known.

11. SUPPLEMENTARY NOTES: Use for additional explanatory notes.

12. SPONSORING MILITARY ACTIVITY: Enter the name of the departmental project office or laboratory sponsoring *(paying for)* the research and development. Include address.

13. ABSTRACT: Enter an abstract giving a brief and factual summary of the document indicative of the report, even though it may also appear elsewhere in the body of the technical report. If additional space is required, a continuation sheet shall be attached.

It is highly desirable that the abstract of classified reports be unclassified. Each paragraph of the abstract shall end with an indication of the military security classification of the information in the paragraph, represented as *(TS)*, *(S)*, *(C)*, or *(U)*.

There is no limitation on the length of the abstract. However, the suggested length is from 150 to 225 words.

14. KEY WORDS: Key words are technically meaningful terms or short phrases that characterize a report and may be used as index entries for cataloging the report. Key words must be selected so that no security classification is required. Identifiers, such as equipment model designation, trade name, military project code name, geographic location, may be used as key words but will be followed by an indication of technical context. The assignment of links, rules, and weights is optional.